

UNCLASSIFIED

AD 408 489

DEFENSE DOCUMENTATION CENTER

FOR

SCIENTIFIC AND TECHNICAL INFORMATION

CAMERON STATION, ALEXANDRIA, VIRGINIA



UNCLASSIFIED

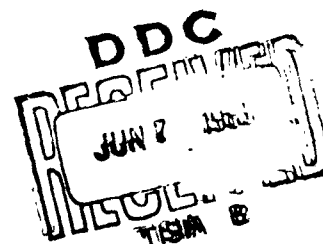
NOTICE: When government or other drawings, specifications or other data are used for any purpose other than in connection with a definitely related government procurement operation, the U. S. Government thereby incurs no responsibility, nor any obligation whatsoever; and the fact that the Government may have formulated, furnished, or in any way supplied the said drawings, specifications, or other data is not to be regarded by implication or otherwise as in any manner licensing the holder or any other person or corporation, or conveying any rights or permission to manufacture, use or sell any patented invention that may in any way be related thereto.

CATALOGED BY DDC  
AS AD No. 408489

408 489

63 4-2472  
22

Qualified requesters may  
obtain copies of this  
report from ASTIA.



AiResearch Manufacturing Division  
Los Angeles 9, California



## ABSTRACT

This total program is directed toward development of a fixed boundary, shell-and-tube, gas-to-air recuperator, for a turboshaft gas turbine aircraft engine, with 2000 hours design life. The object of Phase I of this recuperator development program is engineering design, fabrication, and testing of full scale, 60 degree arc test sections and other required test specimens.

Two different recuperator test sections were fabricated and tested. One was a U-tube unit with compressed air flowing through tubes and exhaust gas flowing over tubes (EOT). The other was a straight tube unit with exhaust gas flowing through tubes and compressed air flowing over tubes (EIT). Both units satisfactorily met the intended performance and environmental requirements. A total of 55.2 hours of operation was accumulated on the (EOT) section and 57 hours on the (EIT) section.

Based on considerations of reliability, life, cost, producibility, and dimensional compatibility with potential engine installations, the configuration with exhaust gas inside tubes has been selected for further evaluation in Phase II of this program. In Phase II, the configuration with exhaust gas inside tubes (EIT) will be fabricated in an annular tube bundle and subjected to an endurance test evaluation. The program, to date, has demonstrated that tubular heat exchanger designs can be used to recuperate turboshaft engines within the requirements for ASW aircraft.

Included in this report are generalized performance curves which may be used to size recuperators for specific engine conditions.

## TABLE OF CONTENTS

<u>SECTION</u>	<u>PAGE</u>
1. INTRODUCTION	1
2. PROBLEM DEFINITION	2
3. TEST UNITS	7
4. HEAT TRANSFER TESTS	21
5. STRUCTURAL TESTS	35
6. PARAMETRIC STUDY	54
7. RECUPERATOR DESIGN	59
8. SUMMARY	70
9. PHASE II PROGRAM	71
10. NOMENCLATURE	72

## LIST OF TABLES

<u>TABLE</u>	<u>PAGE</u>
2-1 Required Performance, (EOT) Recuperator	3
2-2 Required Performance, (EIT) Recuperator	4
4-1 Performance of (EOT) Recuperator Assembly 178123	24
4-2 Performance of (EIT) Recuperator Assembly X178175	29

## LIST OF FIGURES

<u>FIGURE</u>	<u>PAGE</u>
2-1 Vibration Scan	5
2-2 Recuperator Thermal Transient Inputs	6
3-1 U Tube Recuperated Turbohaft Engine (EOT)	9
3-2 Instrumented and Assembled Recuperator Recuperator Assembly 178123	10
3-3 Partially Assembled Core, Recuperator Assembly 178123	11
3-4 Tape Controlled Support Plate Drilling Recuperator Assembly 178123	13

# LIST OF FIGURES (continued)

<u>FIGURE</u>		<u>PAGE</u>
3-5	Tube Stacking, Recuperator Assembly, 178123	14
3-6	Vacuum Brazing, Recuperator Assembly 178123	15
3-7	Straight Tube Recuperated Turboshaft Engine (EIT)	17
3-8	Disassembled Recuperator, Recuperator Assembly X178175	18
3-9	Instrumented Core, Recuperator Assembly X178175	19
4-1	Schematic Diagram, Recuperator Performance Test Setup	22
4-2	Test Performance, Recuperator Assembly 178123	26
4-3	Test Performance, Recuperator Assembly 178123	27
4-4	Test Performance, Recuperator Assembly 178123	28
4-5	Test Performance, Recuperator Assembly X178175	31
4-6	Test Performance, Recuperator Assembly X178175	32
4-7	Test Performance, Recuperator Assembly X178175	33
5-1	Test Performance, Start to Cruise Transient Recuperator Assembly 178123	37
5-2	Tube Scratches from Differential Expansion Recuperator Assembly 178123	39
5-3	Lateral Vibration, Recuperator Assembly 178123	40
5-4	Longitudinal Vibration, Recuperator Assembly 178123	41
5-5	Center Support Plate Shift, Recuperator Assembly 178123	44
5-6	Stresscoat Patterns, Recuperator Assembly 178123	46
5-7	Test Performance, Start to Cruise Transient, Recuperator Assembly X178175	48
5-8	Lateral Vibration, Recuperator Assembly X178175	49
5-9	Longitudinal Vibration, Recuperator Assembly X178175	50
6-1	Parametric Study Results, Exhaust Gas Inside Straight Tubes	56
6-2	Parametric Study Results, Exhaust Gas Inside Straight Tubes	57
6-3	Parametric Study Results, Exhaust Gas Inside Straight Tubes	58
7-1	Air and Exhaust Gas, Specific Heat	64
7-2	Number of Heat Transfer Units, Two-pass Cross-Counterflow Both, Fluids Unmixed Throughout	65
7-3	Recuperator Design Curves, Exhaust Gas Inside Straight Tubes	66
7-4	Recuperator Design Curves, Exhaust Gas Inside Straight Tubes	67
7-5	Recuperator Design Curves, Exhaust Gas Outside Plain U-Tubes	68
7-6	Recuperator Design Curves, Exhaust Gas Outside Plain U-Tubes	69
DRAWING 178123 Recuperator Assembly, Test Unit		
DRAWING X178175 Recuperator Assembly, Test		

## SECTION 1

### INTRODUCTION

This report presents the results and evaluation of analysis and testing performed for development of an exhaust gas to compressed air, fixed boundary recuperator for turboshaft gas turbine aircraft engines, during Phase I of Bureau of Naval Weapons Contract N0w 62-0598-c. The design, fabrication and testing of recuperator test sections has been accomplished during Phase I. Steady-state heat transfer and pressure drop tests have been performed as well as simulated engine mechanical and thermal transients associated with a 2000-hour life. This report includes a description and evaluation of this Phase I activity. The program has been conducted by The Garrett Corporation, AiResearch Manufacturing Division in Los Angeles, California from February through July, 1962.

The main fabrication and test portions of this recuperator development program have been confined to shell-and-tube designs with tube bundles forming sectors of circular annuli. Two configurations have been built and tested. The recuperator section with exhaust gas outside U-tubes (EOT) is shown on enclosed Drawing 178123 and Figure 3-1. The recuperator test section with exhaust gas inside straight tubes (EIT) is shown on enclosed Drawing 178175 and Figure 3-6.

Following program phases will consist of fabrication and endurance testing with a complete recuperator including simulated engine ducting and preparation of a final summary report. The complete recuperator to be fabricated in Phase II will be designated as Part 178620-1; therefore, this part number is used in the report title.



## SECTION 2

### PROBLEM DEFINITION

The Phase I Recuperator Development Program has made use of two problem statements which differ only in the pressure drops allotted on the hot and cold sides of the heat exchanger. The structural requirements are the same for both of the recuperator sections thus far produced and tested. During a coordination meeting with the Bureau of Naval Weapons on April 18, 1962, it was decided to consider  $\Delta P/P_{in}$  values as high as 11 per cent. The (EOT) design was already established and therefore, the (EIT) test section was designed for a somewhat higher  $\Delta P/P_{in}$  than the (EOT) design.

The problem statements for the two recuperator test sections are shown on Tables 2-1 and 2-2. Figures 2-1 and 2-2 depict recuperator vibration and thermal transient inputs.

The problem conditions are based on the requirements for a typical turboshaft gas turbine aircraft engine of approximately 2700 horsepower. Section 6, Parametric Study, and Section 7, Recuperator Design, may be used as a design basis for recuperator selection for engines of any size within the range of interest of this program.

TABLE 2-1

REQUIRED PERFORMANCE  
(EOT) RECUPERATORCompressed Air

Effectiveness, dim.	0.7
Flow Rate, lb per sec	11.31
Inlet Total Temperature °R	905
Inlet Total Pressure, psia	78
Core Static Pressure Drop, $\sigma\Delta P$ , psi	1.615
$\frac{\Delta P_a (100)}{P_{a \text{ in}}}$ , per cent	0.9
Maximum Operating Pressure, psia	212
Maximum Pressure Differential, psi	197.3
Proof Pressure at 1050°F, psig	229.3
Burst Pressure at 1050°F, psig	299.3

Exhaust Gas

Flow Rate,* lb per sec	12.13
Inlet Total Temperature, °R	1720
Outlet Static Pressure, psia	14.7
Recuperator Total to Static Pressure Drop, $\sigma\Delta P$ , psi	0.33
$\frac{\Delta P_g (100)}{P_{g \text{ in}}}$ , per cent	5.8
Total $\frac{\Delta P (100)}{P_{\text{in}}}$ , per cent	6.7

Environmental Conditions

Temperature: -65°F to 250°F  
 Humidity: 0 to 100 per cent  
 Vibration: per Figure 2-1  
 Acceleration: Side-----1g  
                   Vertical---10g  
                   Axial-----2g

Start and Thermal Cycles - 750 start up and shut down cycles per Figure 2-2

Life - 2000 hrs

\*Includes JP-4 combustion products based on fuel to air ratio of 0.018

TABLE 2-2

REQUIRED PERFORMANCE  
(EIT) RECUPERATORCompressed Air

Effectiveness, dim.	0.7
Flow Rate, lb per sec	11.31
Inlet Total Temperature, °R	905
Inlet Total Pressure, psia	78
Recuperator Static Pressure Drop,* $\sigma\Delta P$ , psi	8.0
$\frac{\Delta P_a (100)}{P_{a \text{ in}}}$ , per cent	4.5
Maximum Operating Pressure, psia	212
Maximum Pressure Differential, psi	197.3
Proof Pressure at 1050°F, psig	229.3
Burst Pressure at 1050°F, psig	299.3

Exhaust Gas

Flow Rate,**lb per sec	12.13
Inlet Total Temperature, °R	1720
Outlet Static Pressure, psia	14.7
Recuperator Total to Static Pressure Drop, $\sigma\Delta P$ , psi	0.366
$\frac{\Delta P_g (100)}{P_{g \text{ in}}}$ , per cent	6.4
Total $\frac{\Delta P (100)}{P_{\text{in}}}$ , per cent	10.9

Environmental Conditions

Temperature: -65°F to 250°F  
 Humidity: 0 to 100 per cent  
 Vibration: per Figure 2-1  
 Acceleration: Side-----1g  
                   Vertical----10g  
                   Axial-----2g

Start and Thermal Cycles - 750 start up and shut down cycles per Figure 2-2

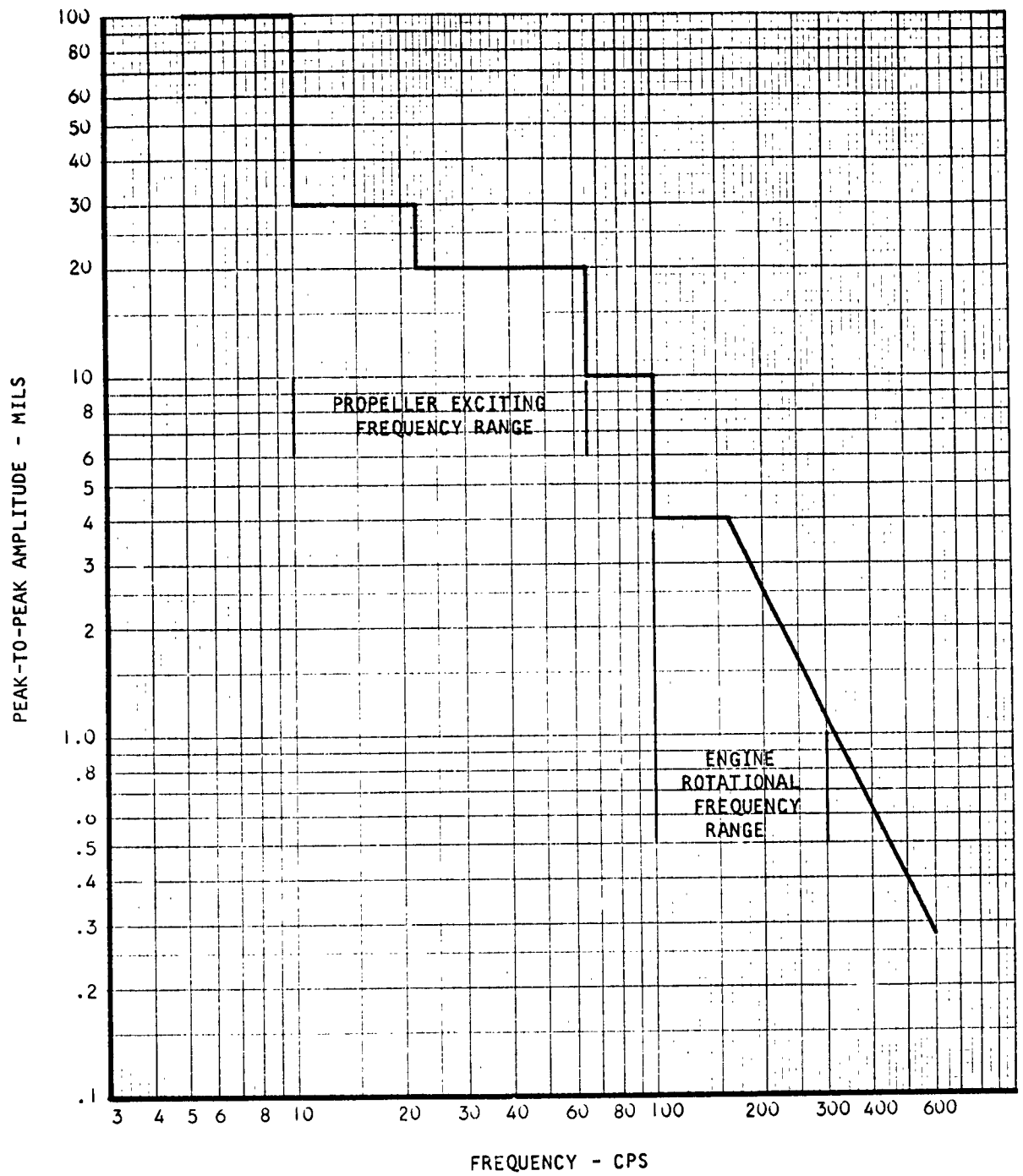
Life - 2000 hrs

\*Includes ducting between engine and recuperator as well as recuperator manifolds.

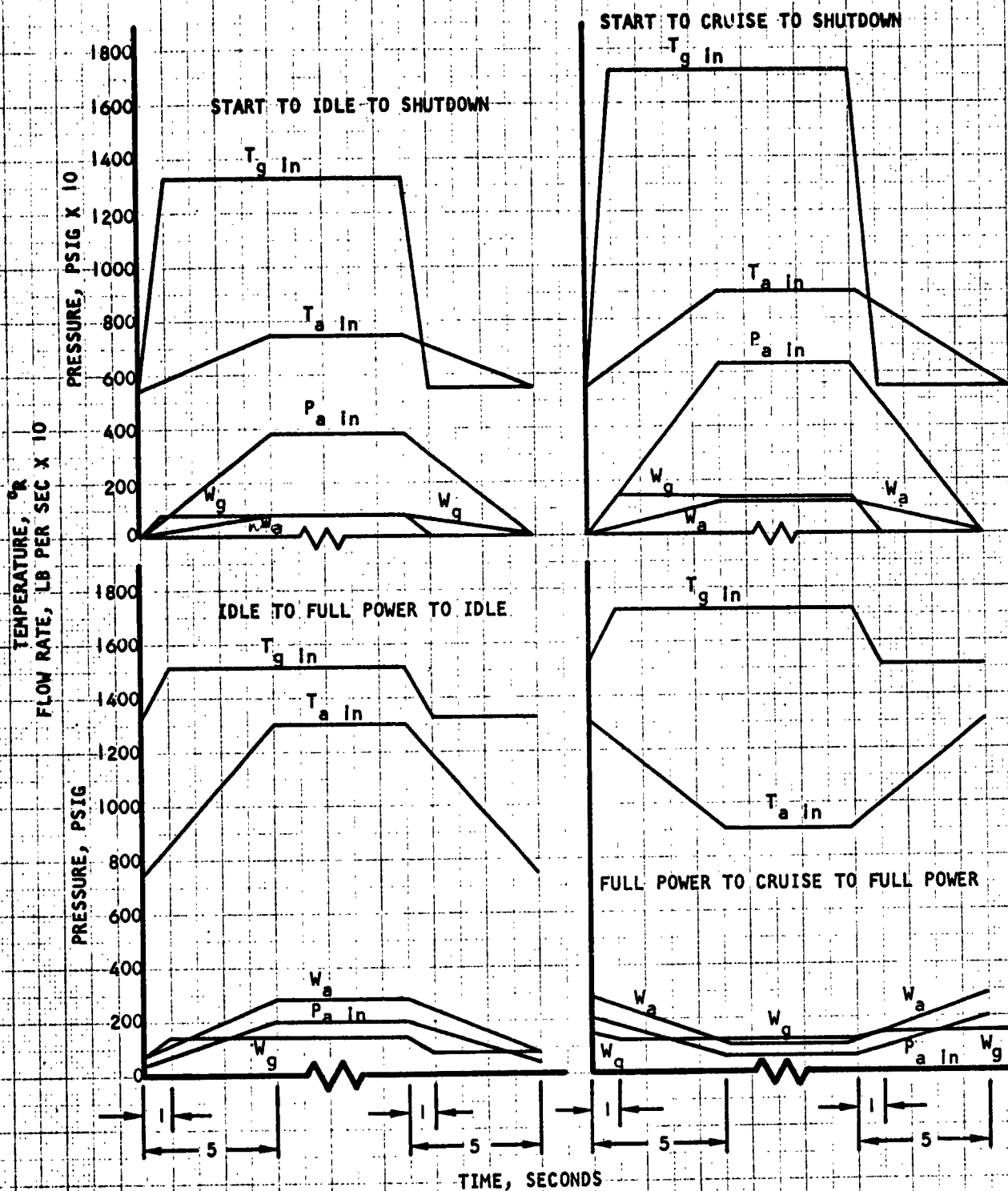
\*\*Includes JP-4 combustion products based on fuel-to-air ratio of 0.018.

L-9149-R

Page 4



PREPARED		8-62	VIBRATION SCAN	FIGURE 2-1
WRITTEN				
APPROVED				
			AIRESEARCH MANUFACTURING CO. LOS ANGELES, CALIFORNIA	



CALCULATED BY				RECUPERATOR THERMAL TRANSIENT INPUTS	FIGURE 2-2
TRACED BY					
CHECKED BY					
APPROVED BY				AIRESEARCH MANUFACTURING CO.	
UNIT NO.				LOS ANGELES CALIFORNIA	



Airesearch Manufacturing Division  
LOS ANGELES 48 CALIFORNIA

### SECTION 3

#### TEST UNITS

Two heat transfer surface types were fabricated for test evaluation. Prior to selection of these particular heat transfer surface types, all types of fixed boundary matrices were considered. During the course of the analysis of these various heat transfer matrices, factors such as weight, size, shape, installation problems, cost, reliability and maintenance were considered. With all of these factors considered, round tubular units provided the best combination of these factors.

Many general considerations applied to both of the configurations selected. Examination of turboshaft engine configurations have shown that the cores for a tubular recuperator could be laid out in an annulus. The structural loads would be carried out at the airframe and the concept provided an internal passage in the center of the core to provide exhaust bypass if desired. Through use of a bypass (open at high load; closed at reduced load), the heat exchanger size and weight can be reduced by designing for effectiveness at the reduced load where improved cycle efficiency is needed. In running at full load, where efficiency is relatively unimportant, the exhaust gas can be diverted as required to avoid overloading.

The actual determination of flow configuration was based on what appeared to be most logical commensurate with engine design. To reduce bulk, it seemed likely that the recuperator core should surround the turbine exit so that the gas flow would be deflected through the core in one pass and discharged aft in the normal manner from the nacelle. The compressor delivery air would flow in two passes counter to the turbine exhaust gas flow path permitting reasonable locations for attaching the compressor and combustor ducting. Not only does this provide a satisfactory packaging arrangement, but a two pass cross counterflow heat exchanger design provides efficient heat transfer within size and weight requirements. The outside diameter was restricted to a maximum of 40 inches and the inside diameter was held to a minimum of approximately 16 inches.

It was decided that the tubes should be oriented in the longitudinal direction in order to provide fairly good structural integrity and permit use of toroidal or flat disc tube sheets, baffle and support plates. Although no mounting devices were necessary for the recuperator test sections, manifolds in the shape of a cylindrical arc segment at the outside radius of the test sections could serve as the point of attachment for radial supports to the engine. The longitudinal location of these radial supports may be varied according to the specific engine installation requirements. These radial supports could take the form of a number of trunions or turnbuckles with attach points on both the recuperator outside shell and the engine. The most appropriate longitudinal location for these radial supports will probably be 6 to 15 inches aft of the forward tube sheets on either design.

Various methods were tried to simplify the tube hole pattern in this special case where the air flow was directed radially outward through the tube bundle. Finally, a modified geometric curve was selected along which holes were placed, and a spacing was selected that maintained the minimum air gap between tubes at any point in the matrix to yield the value desired for heat transfer and friction factor.

It is probable that compressed air will flow through ducts from the engine compressor to the complete recuperator and from the recuperator to the combustion chambers. These ducts will be sized to fit the application flow rate and allowable pressure drop. The single inlet and outlet duct of 5 inch diameter on the compressed air side of both test sections is thought to be a realistic simulation of a full-scale unit.

#### (EOT) Recuperator

The outline configuration of the (EOT) recuperator is shown on Drawing 178123. Figure 3-1 illustrates schematically this design as it would appear installed on a turboprop engine. Figure 3-2 shows the complete test section and Figure 3-3 shows the partially assembled core. This type of design carries the air between the compressor and combustor through tubes having U-bends with the exhaust gas directed radially outward across the tubes. Since the main support was considered to be at the engine, the tube sheets were formed as toroids and reinforced by gussets. The tubes were

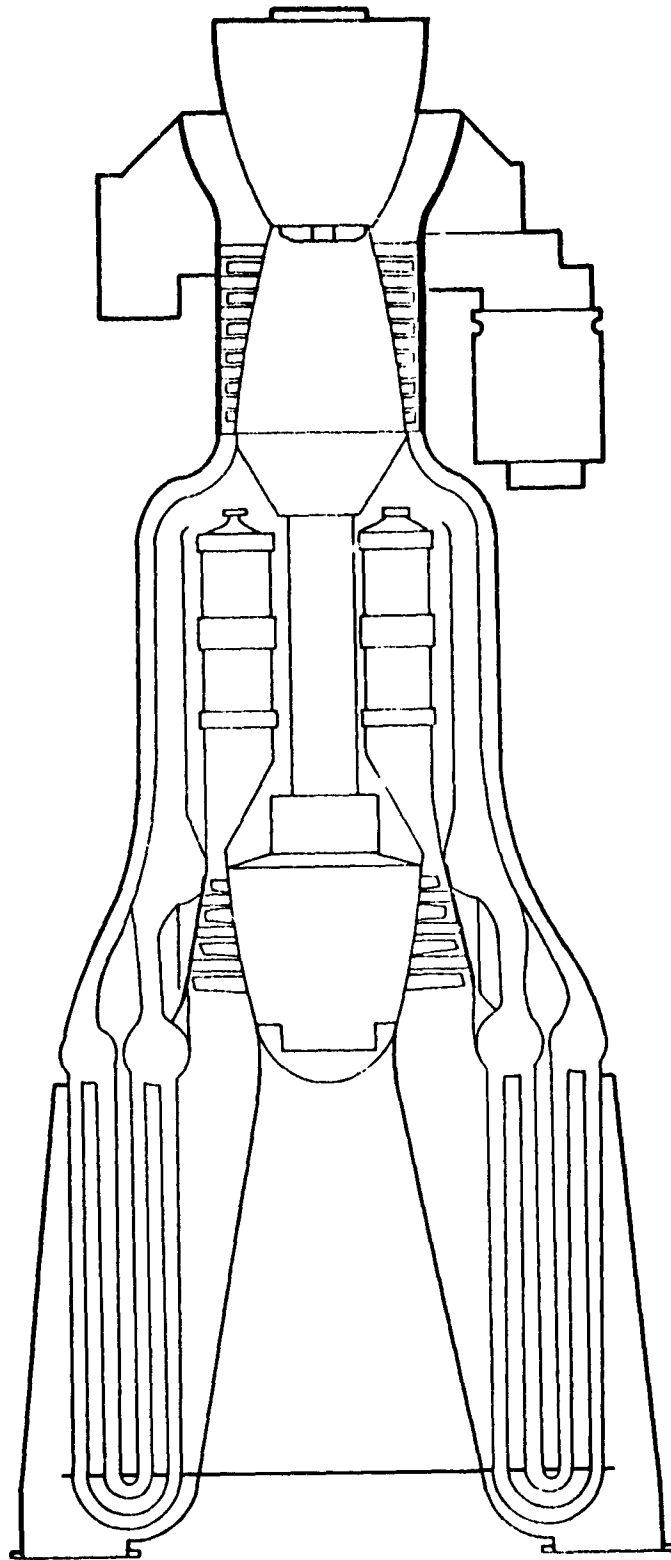


FIGURE 3-1

U TUBE RECUPERATED TURBOSHAFT ENGINE (EOT)





FIGURE 3-2  
INSTRUMENTED AND ASSEMBLED RECUPERATOR  
RECUPERATOR ASSEMBLY 178123

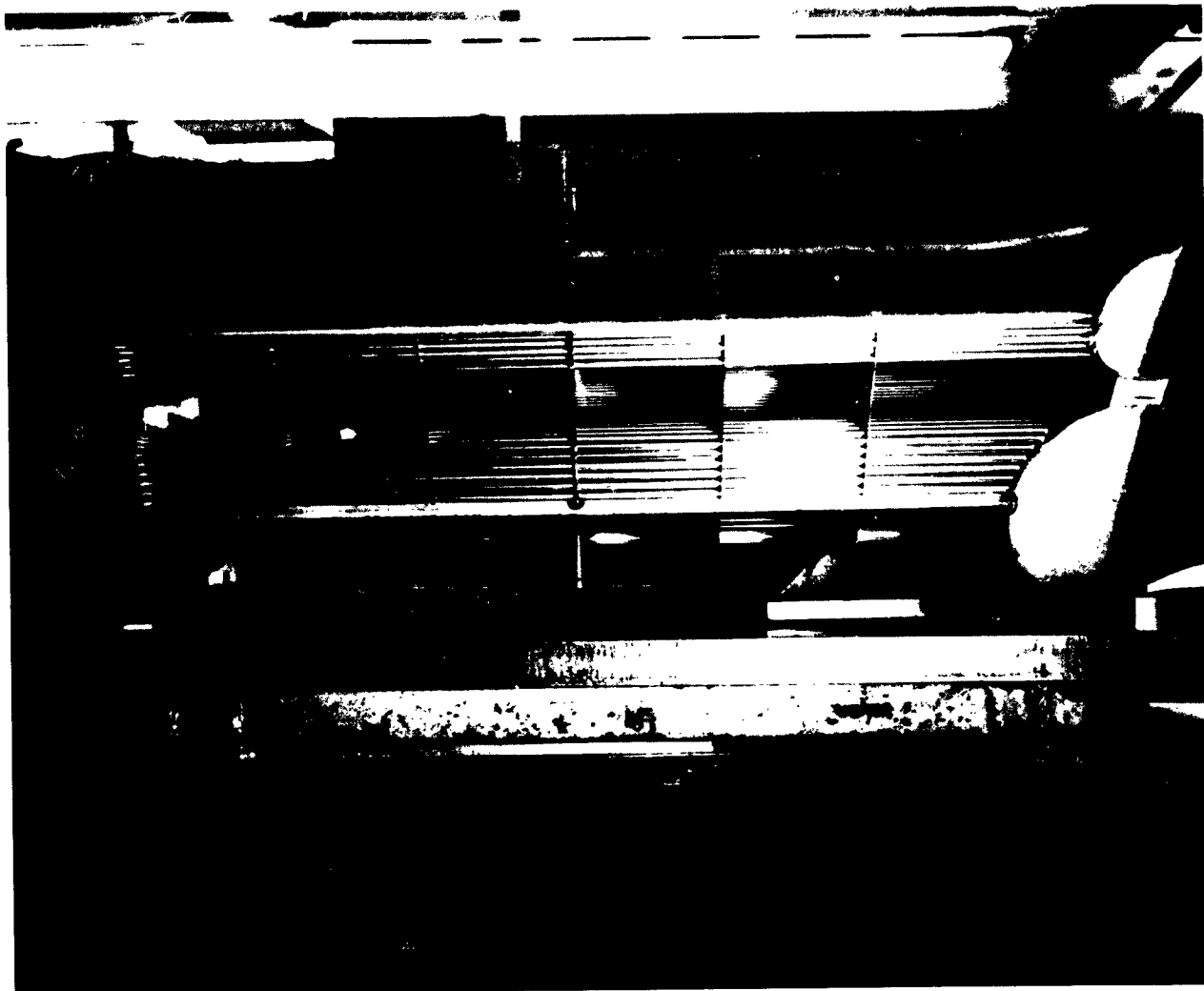


FIGURE 3-3  
PARTIALLY ASSEMBLED CORE  
RECUPERATOR ASSEMBLY 178123

cantilevered from these combinations of duct and support structure. The tubes were arranged according to metal temperature difference such that the tubes subjected to the higher temperature differentials were formed with the larger radii. The transient effects of engine startup and load changes were considered to impose the highest loads on the structure.

The tube sheets were made toroidal in configuration to provide a lightweight unit while maintaining adequate structural integrity for the loads imposed. The tube bundle has two major support plates: one at midspan and the other at the aft end just forward of the U-bend. These plates support the exhaust gas outer manifolding but are not brazed to any of the tubes. This allows free expansion of the U-bends. The aft support plate also supports the inner exhaust gas duct. The four tube spacer plates, located at a uniform spacing between the support plates, were brazed to the tubes which have U-bends of largest radius. The tube bundle support and spacer plates provide radial support for the core and also prevent the tube natural vibration frequency from falling into the propeller excitation and engine rotational frequency ranges.

A 10 degree arc section of the core was constructed of aluminum to establish basic heat transfer and pressure drop characteristics. Analysis of the data showed good correlation with predicted values and confirmed the choice of hole spacing. A full scale, 60 degree arc test section was then designed and fabricated using thin gauge type 304 stainless steel tubing and sheet metal. Brazed and welded construction was used. Satisfactory U-bends were made down to one inch radius. The section was 16 inches ID, 38 inches OD and contained 840, 0.210 in. outside diameter U-tubes which were an average of 26.7 inches between the toroidal tube sheets and the aft support plate. The hole pattern of the tube sheets, baffles and support plates were drilled with a tape-controlled jig borer. The tape was prepared from a computer analysis of the geometrically defined spacing. Figure 3-4 shows the tape drilling operation.

Figures 3-5 and 3-6 respectively show core stacking and core vacuum brazing operations.

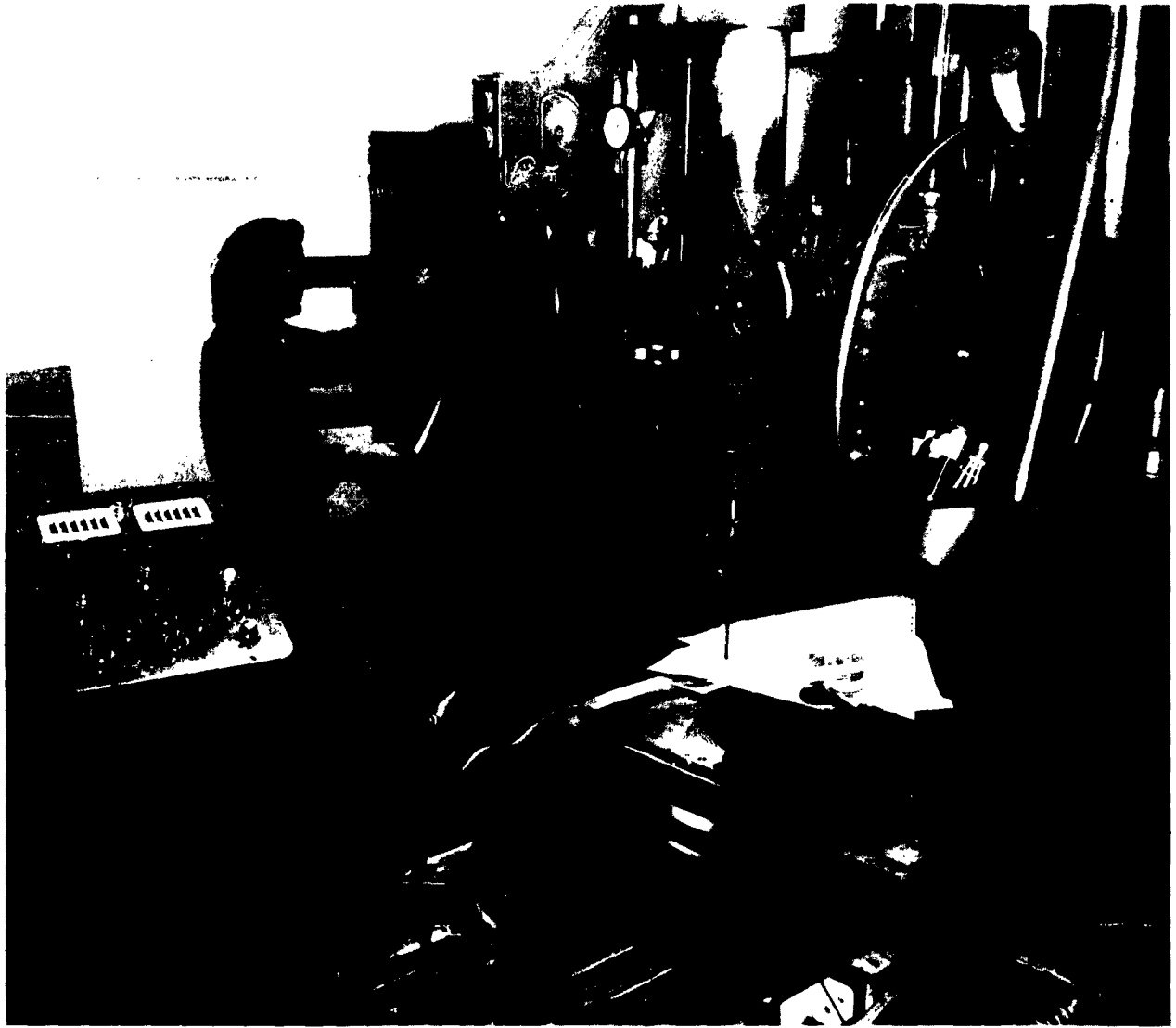


FIGURE 3-4  
TAPE CONTROLLED SUPPORT PLATE DRILLING  
RECUPERATOR ASSEMBLY 178123



FIGURE 3-5  
TUBE STACKING

RECUPERATOR ASSEMBLY 178123

L-9149-R  
Page 14

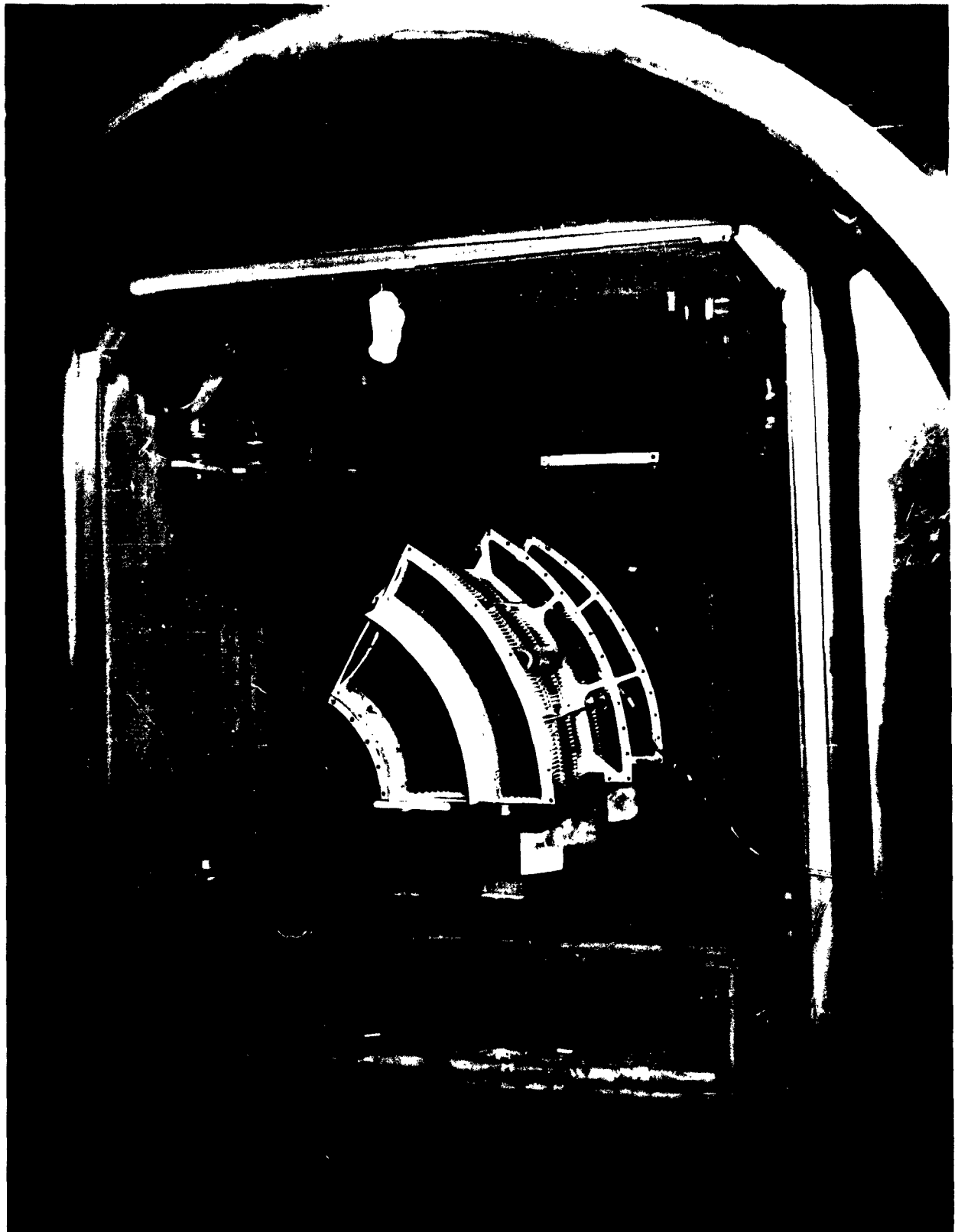


FIGURE 3-6  
VACUUM BRAZING  
RECUPERATOR ASSEMBLY 178123

L-9149-R  
Page 15

### (EIT) Recuperator

The outline configuration of the (EIT) recuperator is shown on Drawing X 178175. Figure 3-7 illustrates schematically this design as it would appear installed on a turboprop engine.

This unit was developed utilizing straight tubes with flat tube sheets. The flow orientation of the U-tube design, with air inside the tubes making two passes crosscounter to the exhaust gas flowing outside the tubes, was known to be a problem using flat tube sheets because of tube sheet stresses resulting from pressure forces and differential temperatures. Also, even if one would consider a straight tube unit with return manifolds replacing the U-bends, a source of structural vibration and bending moments would exist in the manifold required to turn the air from the first into the second pass. Accordingly, it was decided to direct the air around the tubes and the exhaust gas inside the tubes. Figure 3-8 shows the recuperator assembly and Figure 3-9 the core instrumentation. With this concept, air leaving the compressor is directed through an outer casing into the rear half of the tube bundle, is turned into the front half of the tube bundle by an inner duct and is returned to the combustor through an inner duct concentric to the outer casing. Analysis indicated that the metal temperatures in this design tend to equalize throughout the core structure such that a rigid tube bundle would be essentially free of radial stresses due to temperature differences.

It was found in preliminary design that the tubes could be made shorter with this flow arrangement than with the U-tube design, thus reducing overhung bending moments and bulk; also, a particular tube geometry was developed to further reduce tube length.

Core sections were again constructed and tested to establish basic heat transfer and flow friction data for the tube geometry selected. A series of tests were also run to establish susceptibility of tubing to collapsing under external pressure. The tests showed that, while tube wall thickness and diameter are particularly of concern from the standpoint of instability, any reasonable tube diameter that would be considered for units used in aircraft would be so small that collapsing resistance would be very high.

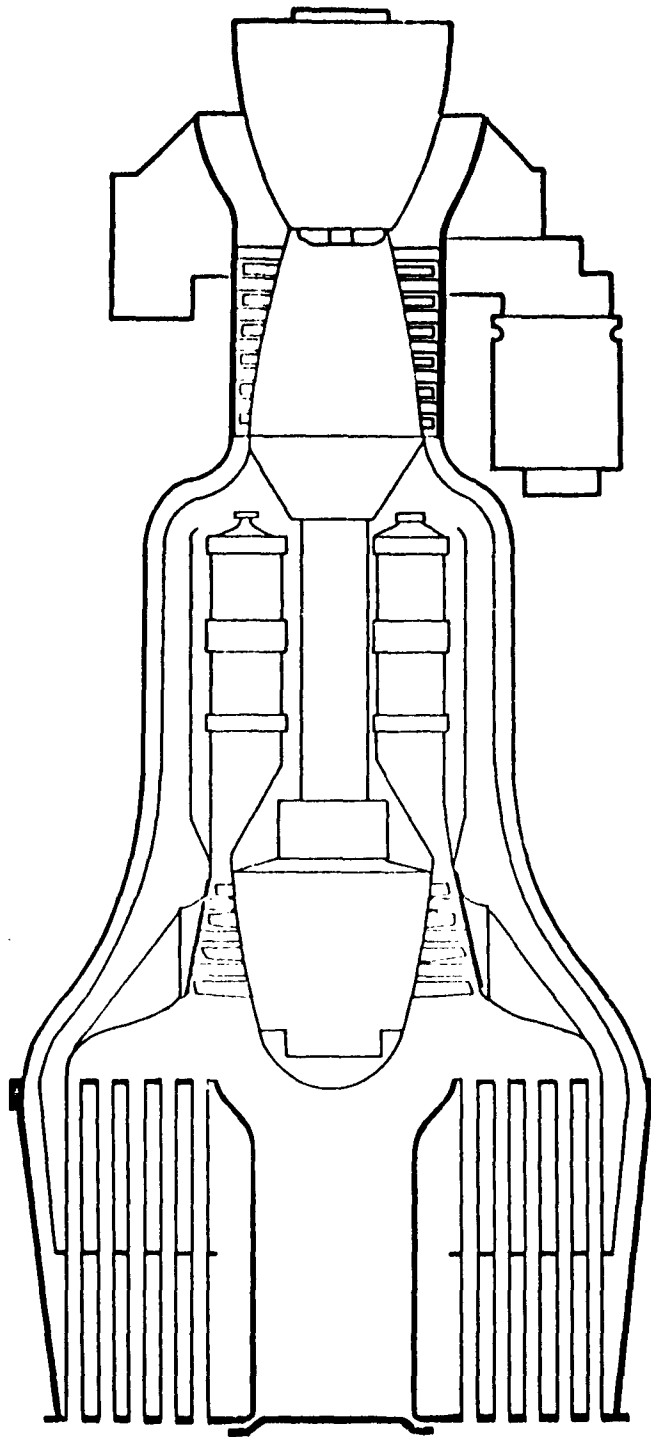


FIGURE 3-7

STRAIGHT TUBE RECUPERATED TURBOSHAFT ENGINE (EIT)



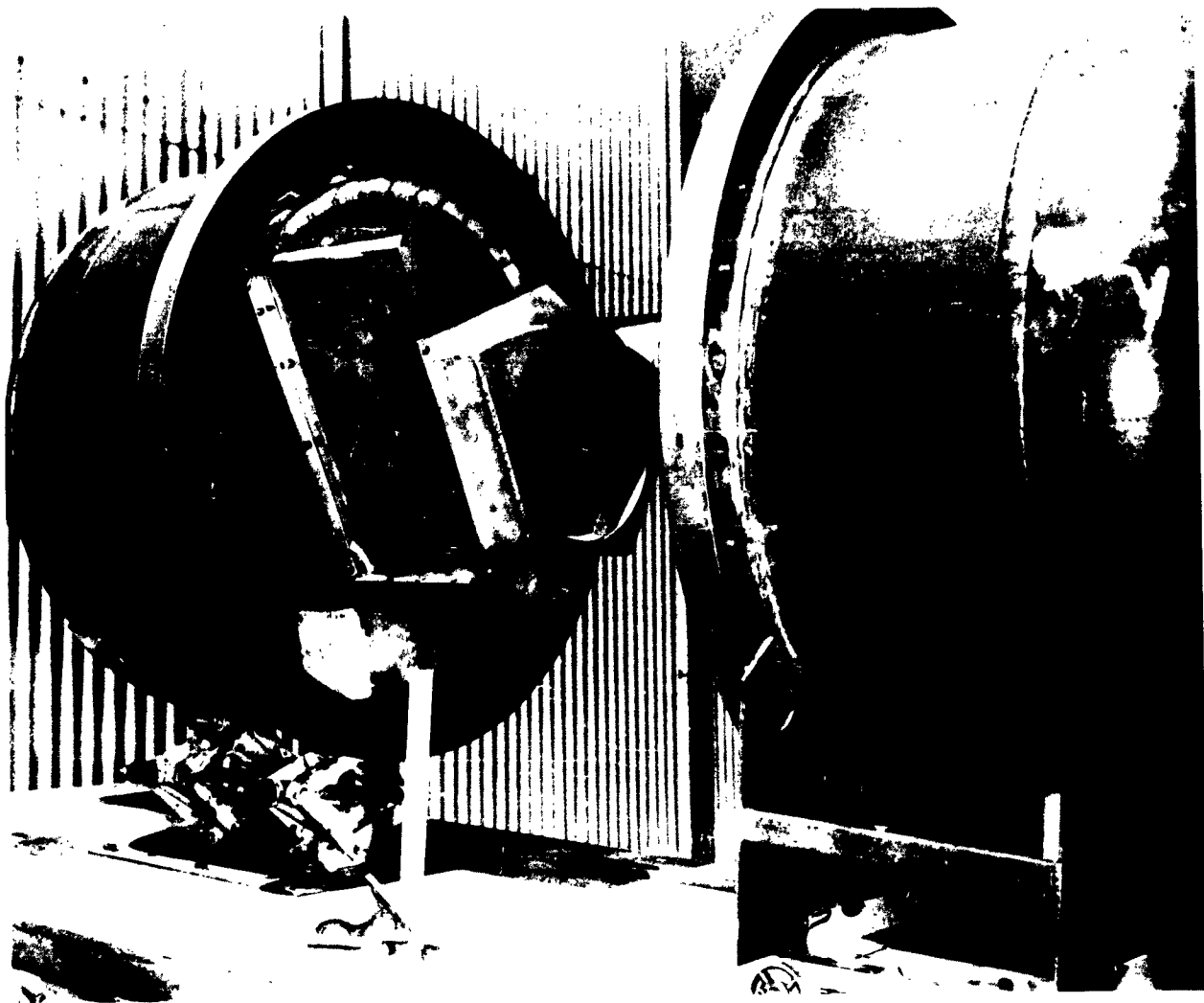


FIGURE 3-8  
DISASSEMBLED RECUPERATOR  
RECUPERATOR ASSEMBLY X178175

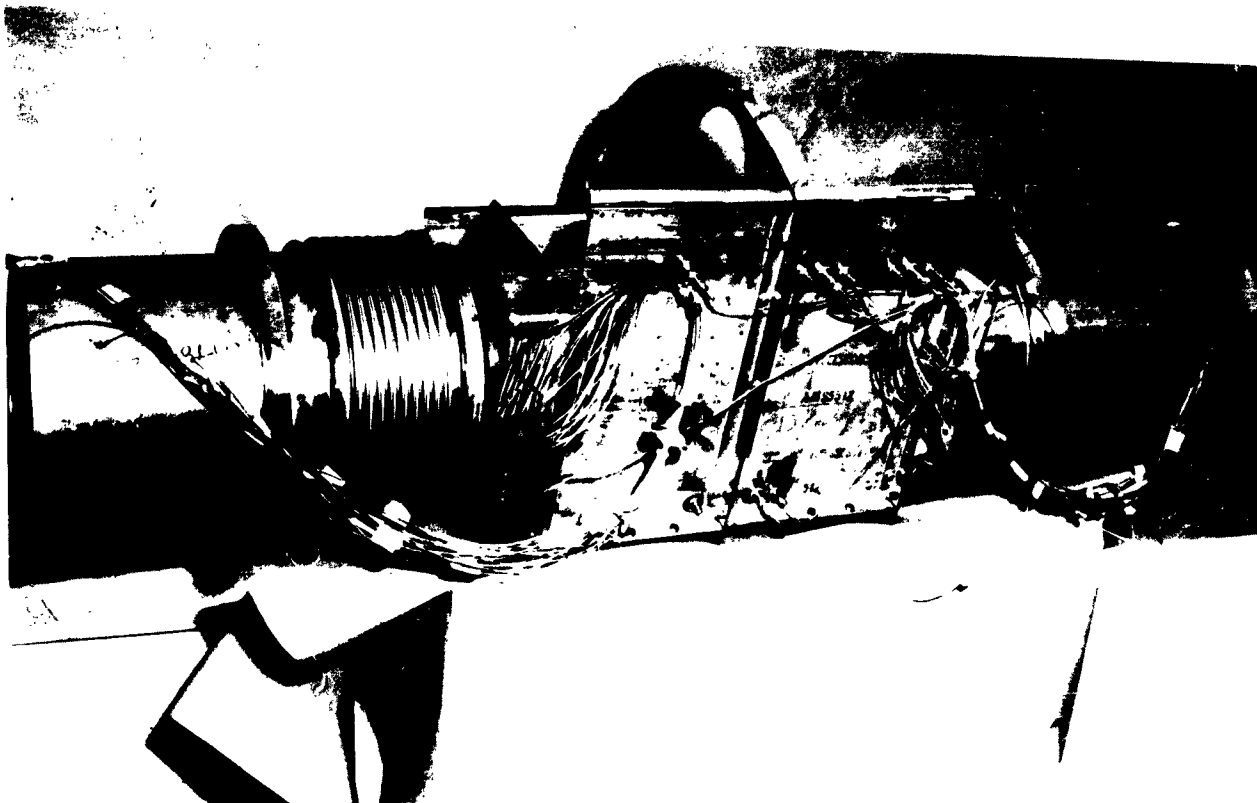


FIGURE 3-9  
INSTRUMENTED CORE  
RECUPERATOR ASSEMBLY X178175

A full scale test section of 60 degrees of arc, 16 inches ID, 35 inches OD, 18.6 inches between tube sheets, and containing 1422, 0.250 inch outside diameter tubes was fabricated from type 347 stainless steel by use of brazed and welded construction. As before, the hole pattern, with adjustment for the slightly larger tube diameter, was designed from computer analysis of the geometrically defined spacing. A baffle plate and spacer plates were used to provide radial support for the core and also prevent the tube natural vibration frequency from falling into the propeller excitation and engine rotational frequency ranges. The core assembly (consisting of tube sheets, tubes, baffle plate and spacer plates) is welded to plenum-type exhaust gas manifolds which are, in turn, connected to expansion bellows and thence to 11-inch diameter inlet and outlet exhaust gas ducts (Figure 3-9). The compressed air is confined by a heavy pressure vessel (selected as an expedient for testing) and directed through the tube bundle by plates bolted and welded at appropriate places to provide a suitable simulation of the full-scale annular unit mechanical and thermal stresses (Figure 3-8).

For performance tests, the unit was modified to have straight, rigid, sheet metal transition ducts on both air and gas sides for accuracy of heat transfer and pressure drop measurements.

## SECTION 4

### HEAT TRANSFER TESTS

Initial tests with air were conducted on a 10 degree arc aluminum test section with flat plate tube sheets. Items of specific concern were flow distribution outside tubes and the variable tube spacing caused by the annular tube bundle configuration. The results of this test confirmed the preliminary performance estimates for the (EOT) design.

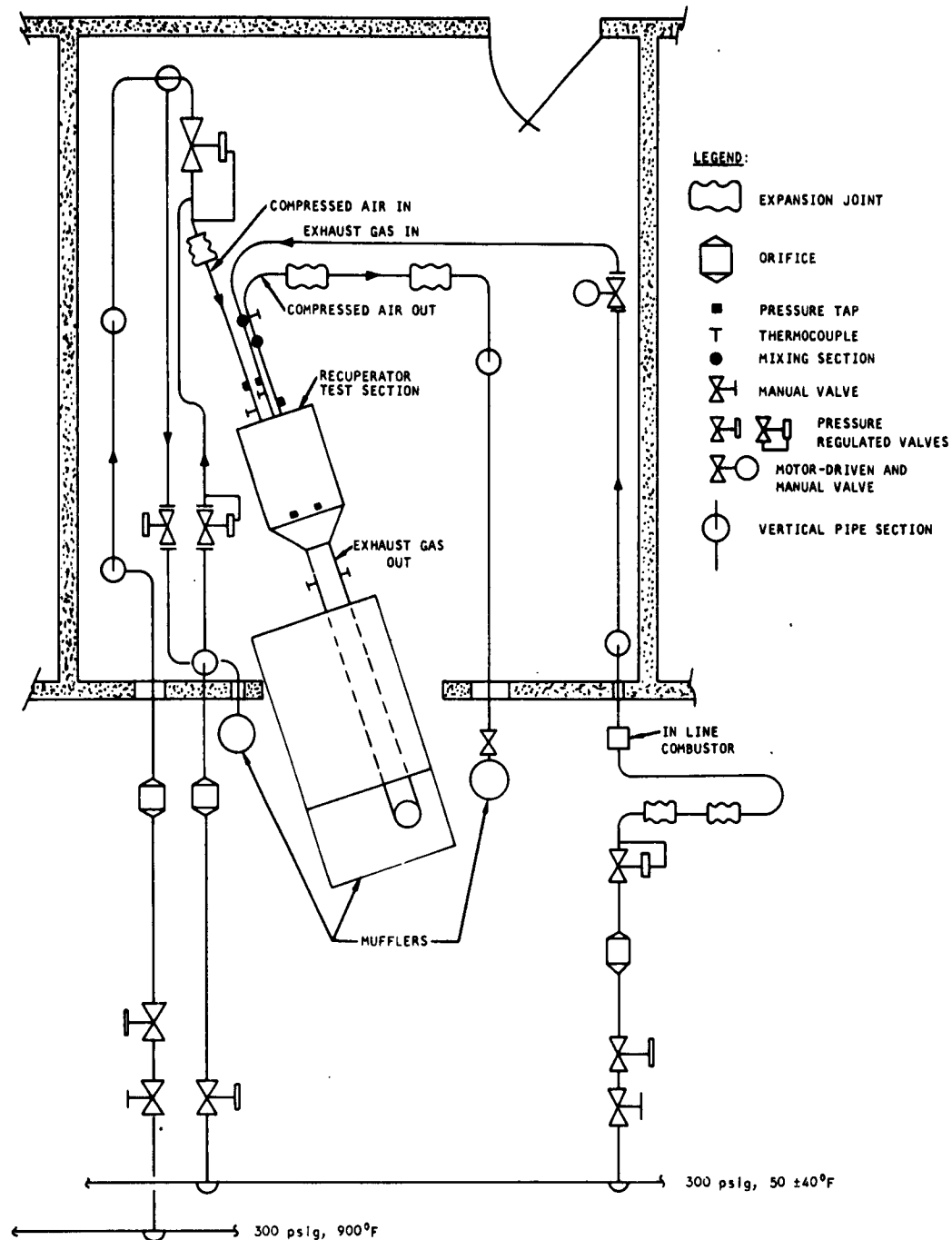
Single steel tubes were tested to determine inside heat transfer coefficient and pressure drop characteristics for tubes used in the (EIT) design. Water was used as the coolant in an annular 3/8 inch pipe jacket. Tests with hot air inside tubes yielded results which allowed size and weight reductions from preliminary (EIT) design estimates. The results from the single tube tests were used in designing the (EIT) test section. (EIT) recuperator test results generally corroborated the single tube tests.

Recuperator Assemblies 178123 and X178175 were tested to determine heat transfer and pressure drop at typical operating conditions. The test setup is shown on Figure 4-1.

Compressed air temperature and flow rate were controlled by mixing the flows from a 900°F and a 50°F, 300 psig source. Exhaust gas was produced by burning JP-4 in an in-line combustor. Combustion air was measured by a single orifice upstream of the combustor. Fuel flow rate was not measured but was calculated from the air flow rate and temperature rise in the combustor by assuming complete combustion and the lower heating value of JP-4 fuel. All orifices were sharp edge, flat plate type.

The thermocouples were chromel alumel and readout was accomplished by use of digital display equipment for the steady state tests and by a multi-channel oscillograph for the transient tests. Pressures and pressure drops were measured by manometers or transducers and read directly or with digital display, depending on the range of values to be read.

The mixing sections consisted of a single piece of pipe placed diametrically through the flow carrying pipe. Typically, a 1.5 inch diametral pipe will be used in a 5 inch pipe. Mixing is produced by high frequency vortex shedding from the diametral pipe.



CALCULATED BY			SCHEMATIC DIAGRAM RECUPERATOR PERFORMANCE TEST SETUP	FIGURE 4-1
TRACED BY				
CHECKED BY				
APPROVED BY				
UNIT NO.			AIRESEARCH MANUFACTURING CO. LOS ANGELES. - CALIFORNIA	

Heat balances were generally from zero to three per cent with scattered points up to five per cent.

#### (EOT) RECUPERATOR

Table 4-1 presents a comparison of design point performance requirements, test performance, and estimated performance based on test performance but at design point conditions of temperature, pressure, and flow rate for (EOT) Recuperator Assembly 178123. Of the parameters listed on Table 2-1, only the flow rates were adjusted to one sixth of their design point value to accommodate the one sixth of a full annulus recuperator test section size.

The agreement between performance estimated from test results and design point requirements is generally good. The resulting effectiveness is higher than design point requirements by an amount which indicates an (EOT) recuperator size reduction of approximately 16 per cent to meet design point requirements. Minor deviations from design point conditions invariably occur during testing due to test parameter tolerances. An exact comparison between design point and test performance is possible only by estimating unit performance at design point conditions but based on test performance. This procedure follows well established principles of fluid mechanics and heat transfer theory which have been repeatedly verified in past tests by AiResearch and others. The effects of viscosity, specific heat, and thermal conductivity on heat transfer coefficients are accounted for. The effect of flow rate and specific heat on capacity rate ratio and number of transfer units is included.

Exhaust gas pressure drop is lower than estimated and compressed air pressure drop higher than estimated with the result that the overall  $\Delta P/P_{in}$  is lower than estimated. Pressure drop is presented as  $\sigma \Delta P$  to allow a direct comparison between all values quoted.  $\Delta P/P_{in}$  is not directly comparable because density effects cannot be properly assessed with this parameter. Static pressure drop is presented for compressed air since this is the parameter measured. Total pressure drop can be more accurately determined by calculation than by measurement, due to the variation in fluid velocity across the stream flowing in a duct. The compressed air

TABLE 4-1  
PERFORMANCE OF  
(EOT) RECUPERATOR ASSEMBLY 178123

<u>Compressed Air</u>	<u>Design Point (Ref. Table 2-1)</u>	<u>Test Performance</u>	<u>Predicted Performance at Design Conditions</u>
Effectiveness, dim.	0.7	0.73	0.733
Flow Rate, lb per sec	1.88	1.88	1.88
Inlet Total Temperature, °R	905	905	905
Inlet Total Pressure, psia	78	78	78
Core Static Pressure Drop, $\Delta P$ , psi	1.615	*	2.0
Recuperator Static Pressure Drop, $\Delta P$ , psi	*	2.5	2.5
$\frac{\Delta P_a(100)}{P_{a \text{ in}}}$ , per cent	0.9	*	1.11
<u>Exhaust Gas</u>			
Flow Rate, lb per sec	2.02**	2.05***	2.02**
Inlet Total Temperature, °R	1720	1547	1720
Outlet Static Pressure, psia	14.7	14.21	14.7
Recuperator Total to Static Pressure Drop, $\Delta P$ , psi	0.33	*	0.253
Recuperator Static to Static Pressure Drop, $\Delta P$ ; psi	*	0.243	0.239
$\frac{\Delta P_g(100)}{P_{g \text{ in}}}$ , per cent	5.8	*	4.45
Total $\frac{\Delta P(100)}{P_{in}}$ , per cent	6.7	*	5.56

\*Not Available

\*\* Includes JP-4 combustion products based on fuel-to-air ratio of 0.018

\*\*\* Includes JP-4 combustion products based on fuel-to-air ratio of 0.015

core static pressure drop is estimated by subtracting one velocity head in the inlet duct and 0.5 velocity head in the outlet duct from the recuperator static pressure drop. These are realistic shock loss assessments for the duct and manifold combination tested. The estimated values of total to static pressure drop for exhaust gas are determined by adding one velocity head in the recuperator inlet duct to the static pressure drop. This method of calculation has proven accurate in previous tests by AiResearch and others. The effects of flow acceleration on pressure drop is included in the performance estimates, although it is a minor factor and accounts for less than 5 per cent of either compressed air or exhaust gas pressure drop.

Figures 4-2, 4-3 and 4-4 show compressed air effectiveness, pressure drop with heat transfer, and isothermal pressure drop, respectively, for Recuperator Assembly 178123. All of the above are plotted as a function of flow rate.

A comparison of Figures 4-3 and 4-4 shows that compressed air pressure drop is higher and exhaust gas pressure drop is lower with heat transfer than with isothermal conditions. This results from changes in boundary layer and flow profile caused primarily by differences in viscosity and density between the two conditions.

The recuperator static pressure drop for both compressed air and exhaust gas includes manifold pressure drop but not extended ducting between the engine and recuperator. The notes on the curves indicate the manner in which the estimated pressure drop curves were produced. The estimates are included to allow a better comparison between design point requirements and test performance.

#### (EIT) RECUPERATOR

Table 4-2 presents a comparison of design point performance requirements, test performance, and estimated performance based on test performance but at design conditions of temperature, pressure and flow rate for (EIT) Recuperator Assembly X178175.

Initial performance tests of (EIT) Recuperator Assembly X178175 resulted in low effectiveness and low compressed air pressure drop. Core



core static pressure drop is estimated by subtracting one velocity head in the inlet duct and 0.5 velocity head in the outlet duct from the recuperator static pressure drop. These are realistic shock loss assessments for the duct and manifold combination tested. The estimated values of total to static pressure drop for exhaust gas are determined by adding one velocity head in the recuperator inlet duct to the static pressure drop. This method of calculation has proven accurate in previous tests by AiResearch and others. The effects of flow acceleration on pressure drop is included in the performance estimates, although it is a minor factor and accounts for less than 5 per cent of either compressed air or exhaust gas pressure drop.

Figures 4-2, 4-3 and 4-4 show compressed air effectiveness, pressure drop with heat transfer, and isothermal pressure drop, respectively, for Recuperator Assembly 178123. All of the above are plotted as a function of flow rate.

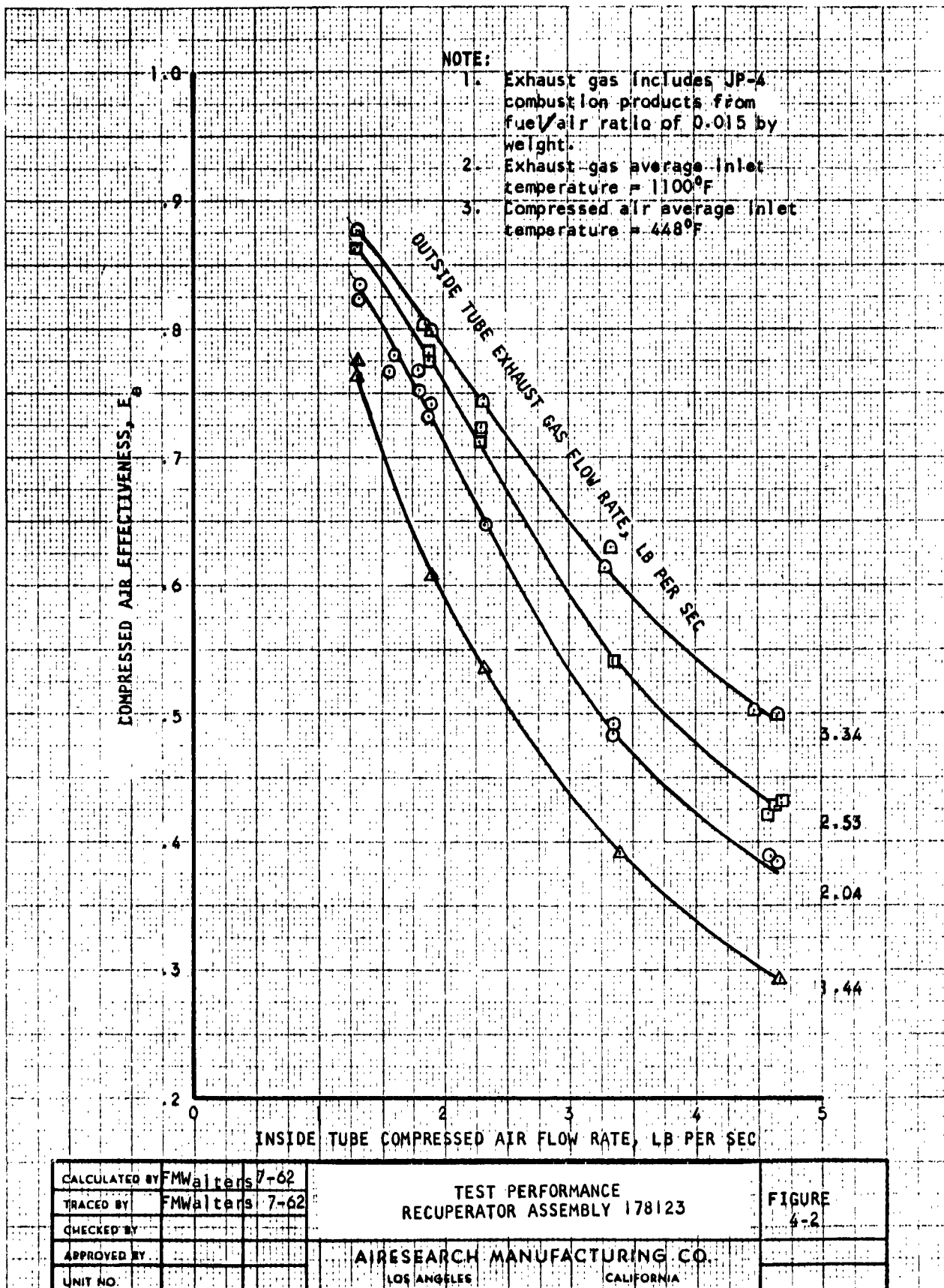
A comparison of Figures 4-3 and 4-4 shows that compressed air pressure drop is higher and exhaust gas pressure drop is lower with heat transfer than with isothermal conditions. This results from changes in boundary layer and flow profile caused primarily by differences in viscosity and density between the two conditions.

The recuperator static pressure drop for both compressed air and exhaust gas includes manifold pressure drop but not extended ducting between the engine and recuperator. The notes on the curves indicate the manner in which the estimated pressure drop curves were produced. The estimates are included to allow a better comparison between design point requirements and test performance.

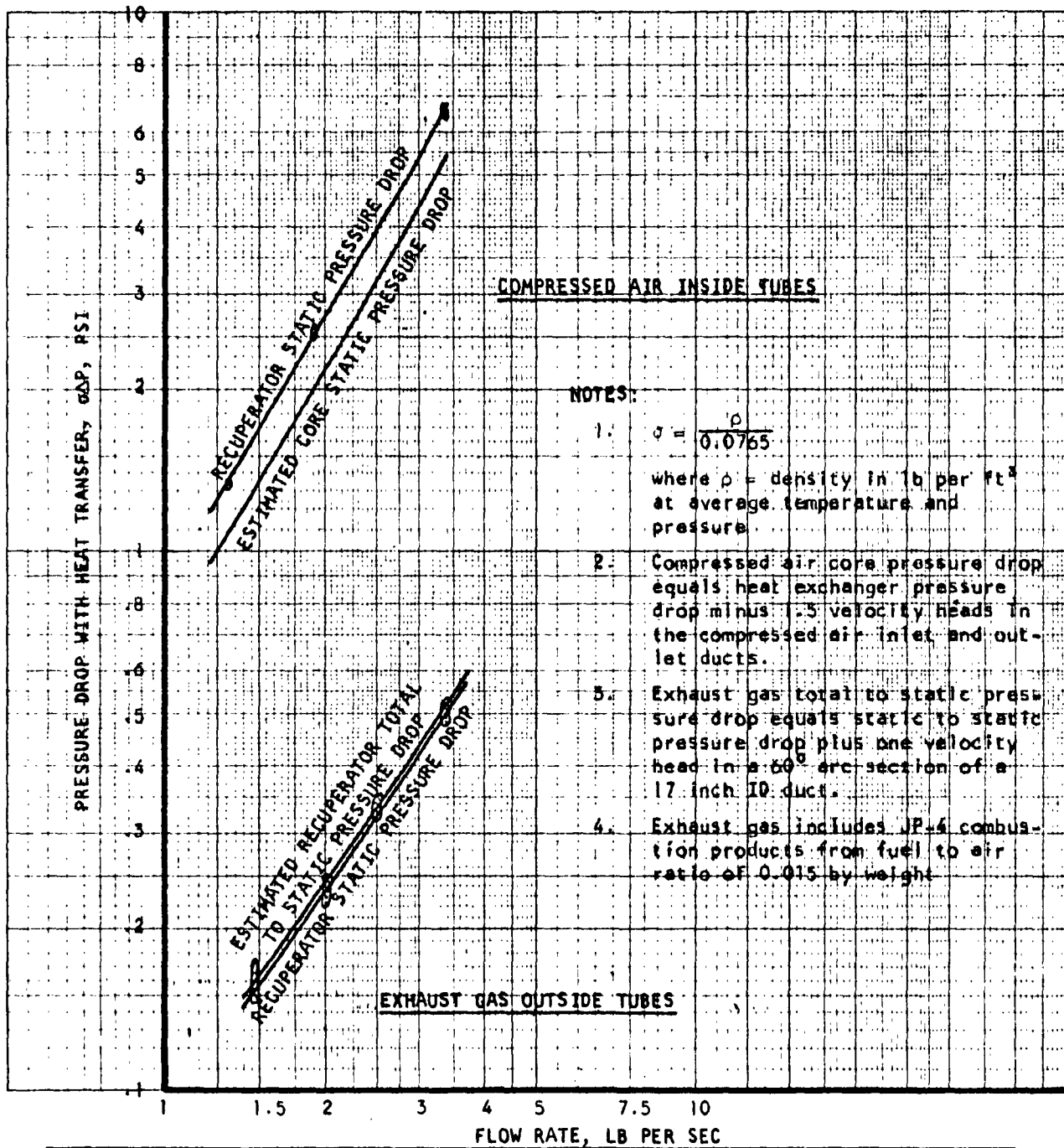
#### (EIT) RECUPERATOR

Table 4-2 presents a comparison of design point performance requirements, test performance, and estimated performance based on test performance but at design conditions of temperature, pressure and flow rate for (EIT) Recuperator Assembly X178175.

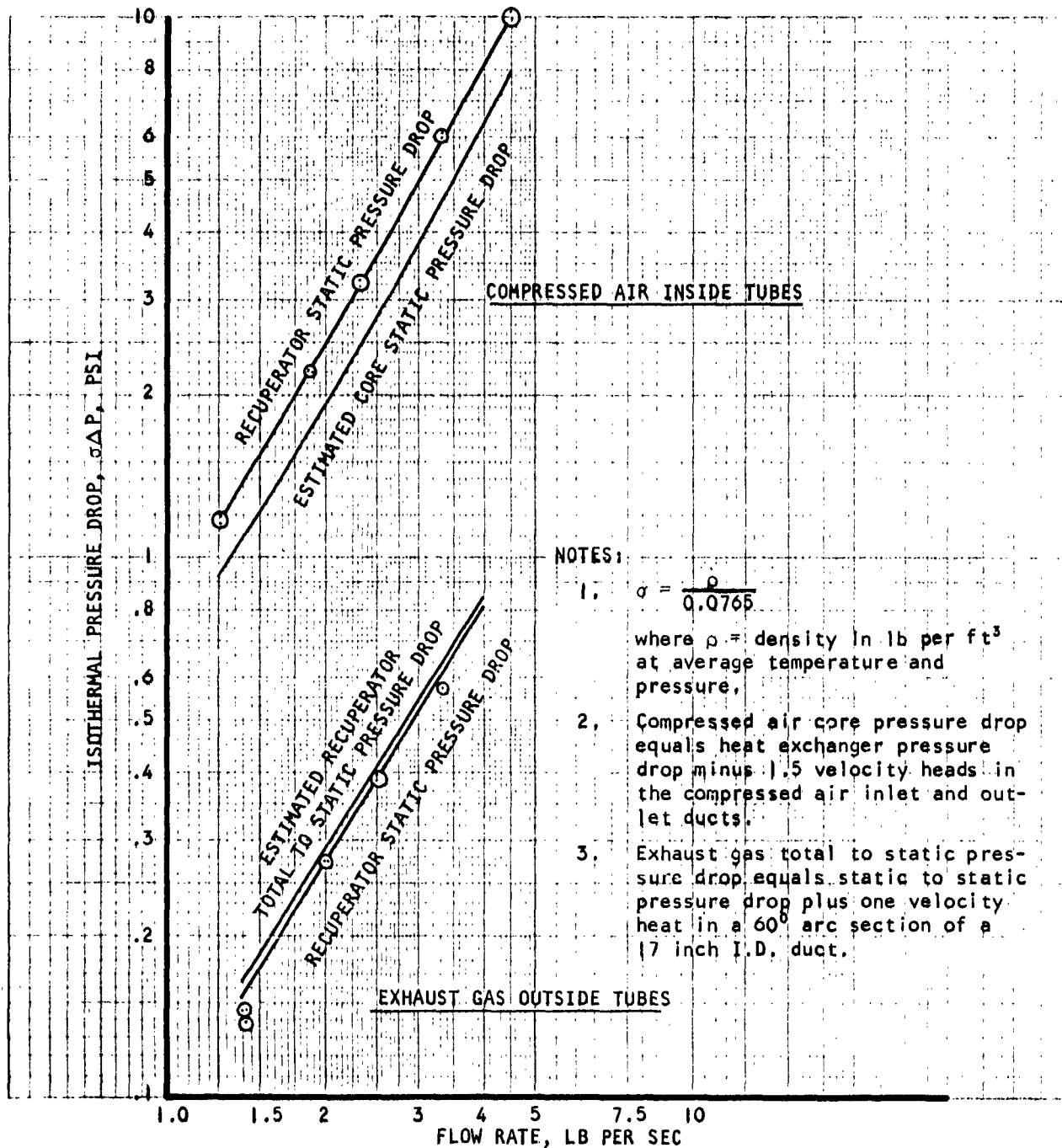
Initial performance tests of (EIT) Recuperator Assembly X178175 resulted in low effectiveness and low compressed air pressure drop. Core



AiResearch Manufacturing Division  
LOS ANGELES 48, CALIFORNIA



CALCULATED BY	Walters	7-62	TEST PERFORMANCE RECUPERATOR ASSEMBLY 178123	FIGURE 4-3
TRACED BY	Walters	7-62		
CHECKED BY			AIRESEARCH MANUFACTURING CO. LOS ANGELES, — CALIFORNIA	
APPROVED BY				
UNIT NO.				



CALCULATED BY	Walters	7-62	TEST PERFORMANCE RECUPERATOR ASSEMBLY 178123	FIGURE 4-4
TRACED BY	Walters	7-62		
CHECKED BY			AIRESEARCH MANUFACTURING CO. LOS ANGELES, — CALIFORNIA	
APPROVED BY				
UNIT NO.				

TABLE 4-2  
PERFORMANCE OF  
(EIT) RECUPERATOR ASSEMBLY X178175

<u>Compressed Air</u>	<u>Design Point (Ref. Table 2-2)</u>	<u>Test Performance</u>	<u>Predicted Performance at Design Conditions</u>
Effectiveness, dim.	0.7	0.677	0.704
Flow Rate, lb per sec	1.88	1.9	1.88
Inlet Total Temp- erature, °R	905	660	905
Inlet Total Pres- sure, psia	78	23.64	78
Recuperator Static Pressure Drop, $\alpha\Delta P$ , psi	8.0*	7.1	7.7*
$\frac{\Delta P_a(100)}{P_{a \text{ in}}}$ , per cent	4.5*	****	4.34*
<u>Exhaust Gas</u>			
Flow Rate, lb per sec	2.02**	2.04***	2.02**
Inlet Total Temp- erature, °R	1720	1050	1720
Outlet Static Pres- sure, psia	14.7	14.49	14.7
Recuperator Total to Static Pressure Drop, $\alpha\Delta P$ , psi	0.366	****	0.305
Recuperator Static to Static Pressure Drop, $\alpha\Delta P$ , psi	****	0.295	0.29
$\frac{\Delta P_g(100)}{P_{g \text{ in}}}$ , per cent	6.4	****	5.33
Total $\frac{\Delta P(100)}{P_{in}}$ , per cent	10.5	****	9.67

\*Includes ducting between engine and recuperator as well as recuperator manifolds

\*\*Includes JP-4 combustion products from fuel-to-air ratio of 0.018

\*\*\*Includes JP-4 combustion products from fuel-to-air ratio of 0.0072

\*\*\*\*Not available

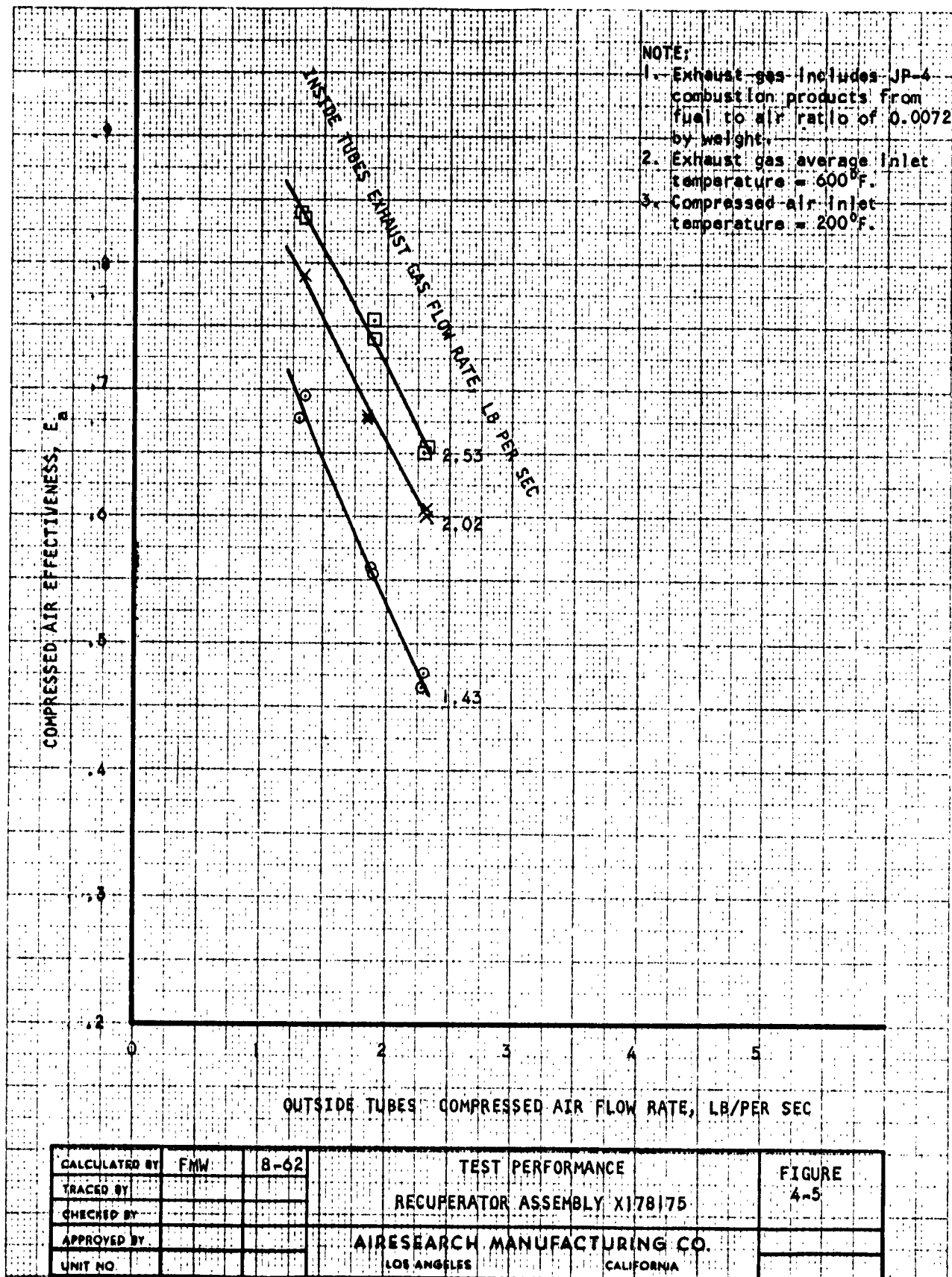
bypassing of up to one-half the air flow was ascertained to be the cause. The recuperator core assembly was removed from the tank and sheet metal manifolds were applied which were both pressure and temperature limited. The temperature limitation was due to the use of epoxy resins to seal joints in the sheet metal manifolds. A retest showed a better but still low effectiveness and pressure drop caused by compressed air passing between the tube bundle and the sheet metal side plates. This air bypassing was essentially eliminated by installing asbestos packing behind stainless steel sheet placed between the side plates and tube bundle, and by reinforcing the side plates from the outside. This configuration was then tested and the performance obtained was essentially as predicted. This problem will not arise in the complete annulus because the side plates will be eliminated and the tube bundle will be continuous.

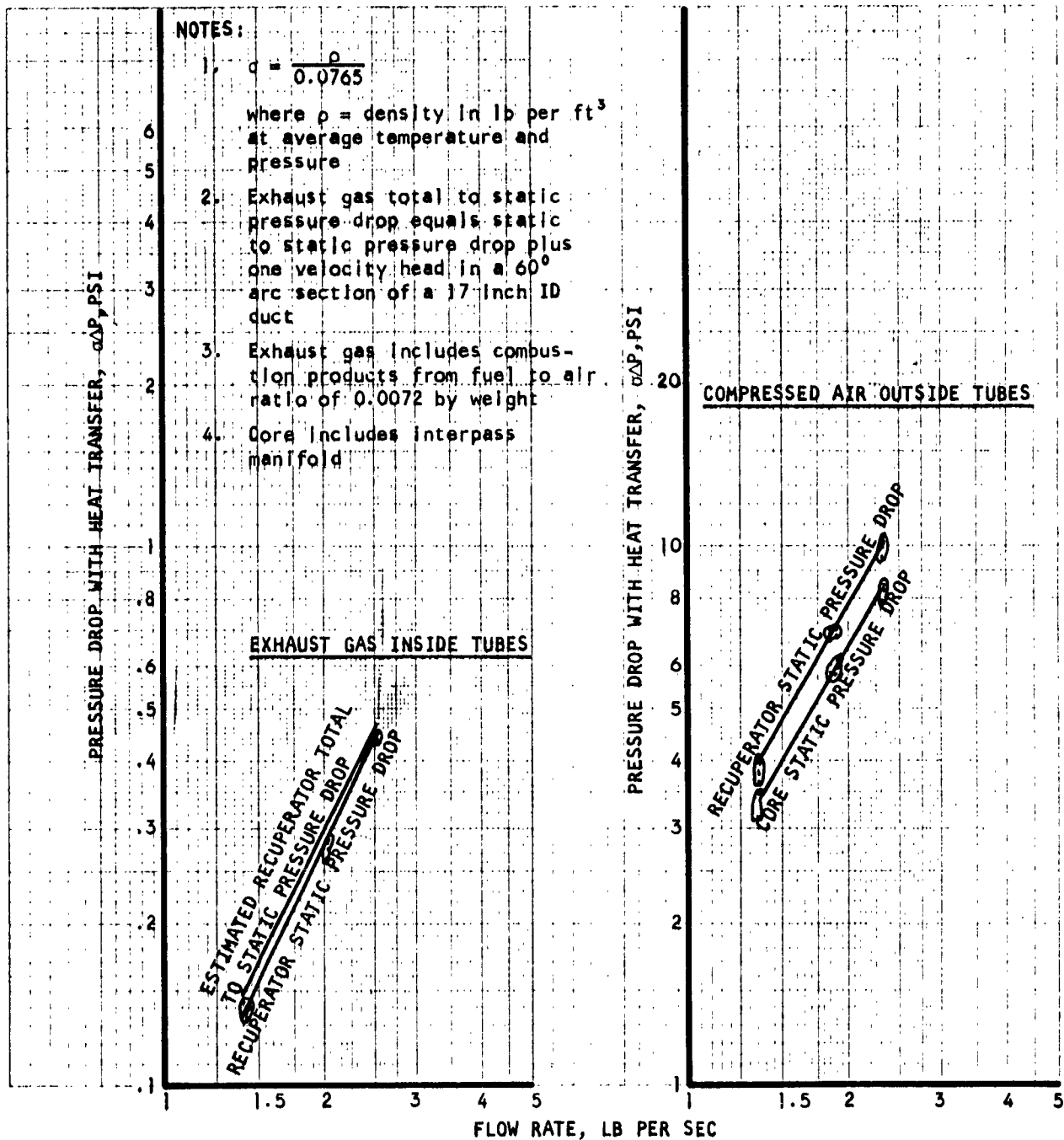
The estimated effectiveness based on test data is fractionally higher than the design point requirement and no recuperator size change is indicated to meet design point requirements. Comments about the effects of temperature on performance and the means for estimating performance at other than test temperatures made for the (EOT) design apply equally to the (EIT) design.

The pressure drop for both exhaust gas and compressed air are slightly below design point values so the total  $\Delta P/P_{in}$  is below the design point value. Recuperator pressure drop generally includes manifolds but not ducting between engine and recuperator. Core pressure drop generally includes no manifolding losses. Exceptions to these rules are noted on the tables or figures. Comments about the pressure drop estimation and presentation methods made for the (EOT) design apply equally to the (EIT) design.

Figures 4-5, 4-6, and 4-7 show compressed air effectiveness, pressure drop with heat transfer, and isothermal pressure drop, respectively, for (EIT) Recuperator Assembly X178175. All of the above are plotted as a function of flow rate.

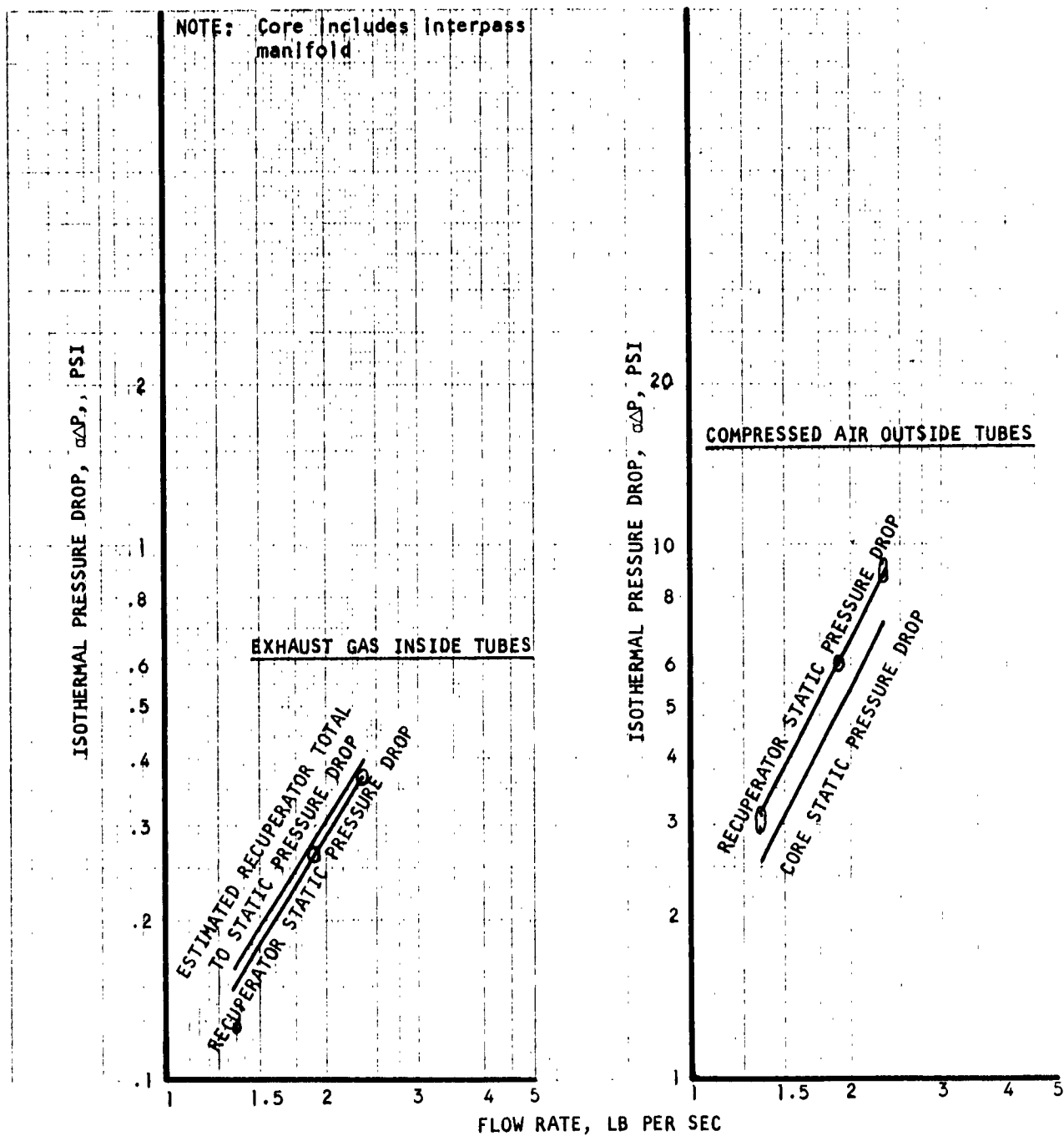
The relation between the pressure drop curves with heat transfer and with isothermal conditions is as stated for the (EOT) design and for the same reasons. Core pressure drop, including the interpass manifold was





CALCULATED BY	Walters	7-62	TEST PERFORMANCE RECUPERATOR ASSEMBLY X178175	FIGURE 4-6
TRACED BY	Walters	7-62		
CHECKED BY			AI RESEARCH MANUFACTURING CO. LOS ANGELES, CALIFORNIA	
APPROVED BY				
UNIT NO				





DESIGNED BY	Walters	7-62
TESTED BY	Walters	7-62
CHECKED BY		
APPROVED BY		
DATE		

TEST PERFORMANCE  
RECUPERATOR ASSEMBLY X178175

FIGURE 4-7

AIR RESEARCH MANUFACTURING CO.  
LOS ANGELES, CALIFORNIA

recorded as test data for the compressed air and is therefore presented. The difference between recuperator and core compressed air pressure drop is approximately three velocity heads based on the inlet and outlet duct diameter of 5 inches. This is higher than estimated for the final design because there is a sharp transition between the ducts and the plenums of the core inlet and outlet.

## SECTION 5

### STRUCTURAL TESTS

#### RECUPERATOR ASSEMBLY 178123 (EOT)

##### Flow Excitation

After the heat transfer tests (Section 4), and before the vibration scan, an air flow rate of 200 lb per min (equivalent to 20 lb per sec for a full size annulus) was passed outside the tubes for 5 minutes. There was no evidence of air flow induced excitation, indicating that fatigue from aerodynamically induced vibration was not likely to be a problem in this design. The spacer plates definitely supported the tubes and the staggered tube arrangement tended to equalize local disturbances.

##### Temperature Measurements - Steady-State and Transient

A series of investigations were run to evaluate the effects of transient engine operating cycles. The unit was instrumented with thermocouples on tubular elements and adjacent structure. The assembly was tested to measure response to engine start to idle, start to cruise, and load changes from idle to full power and cruise to full power. These tests were made at full temperature and pressure, utilizing an inline gas turbine engine combustor to supply the exhaust gas and a laboratory compressed air source for the compressed air side. This facility was designed to simulate the characteristics of engines modeled after Military Specification MIL-E-8593, the general specification for turboprop aircraft engines. The transient input was based on conditions shown on Figure 2-2.

The objective of these tests was, first, to confirm the calculated steady-state temperature distribution, and second, to establish temperature gradients and temperature differentials existing during transient conditions. The most critical steady-state condition is represented by values shown on Table 2-1. This condition yields a severe radial temperature gradient on the support plates and a large temperature differential between corresponding straight sections of the U-tubes. More severe radial temperature differences will exist during the transient startup to cruise condition.

The measured steady-state temperature distribution agreed fairly well with the calculated values. There were no prominent differences that would influence the original theoretical steady-state design concepts. Due to the uncertainty of the thermocouple data giving the true mean metal temperature of tubes, the calculated values have been considered to be more reliable and have been used where a local discrepancy in measured and calculated values exists. There are many factors that can influence the reliability of the thermocouple values: for example, the position of the thermocouple on the tube relative to the flow; the local change in heat transfer characteristics due to the mass of the thermocouple itself and any associated insulation; and, most important of all, the validity of measuring mean metal temperature with a thermocouple junction on the surface.

Examination of the oscillograph traces recorded during start to cruise, start to idle, and idle to full power indicate that some of the most severe transients occur during start to cruise. Typical curves of temperature and pressure variation with time for start to cruise are shown on Figure 5-1. As a fuel control system was not available in the laboratory, the start condition was simulated by establishing gas flow through a bypass before a run was started. The exhaust inlet temperature is shown initially at 1530°R because of bypass valve leakage through the recuperator. This bypass valve leakage was eliminated for the (EIT) transient tests. When recording a startup, the diverter valve was closed and gas was passed through the unit, building up to full conditions in 2 seconds. The compressed air source was timed manually to start its transient 2 to 4 seconds after the start of the test. An automatic programmer mixed cold and hot air flows to simulate the characteristic of an engine compressor during load changes.

The data indicates that transient temperature differentials between the straight sections of the U-tubes of 1.5 times steady-state occur in the outer U-tubes and possibly as high as 2.0 times in the inner U-tubes. The transient in the outer U-tubes is not critical, since these large radius U-bends have sufficient margin to absorb the extra transient growth; however, the inner U-bend radii probably should be increased in future units on the basis of single U-tube tests discussed later in this report.



Differential elongation during thermal cycling caused light scratches on the tubes at the aft support plate, as shown on Figure 5-2. There is a possibility that the outer shell of the test unit expanded more than tubes, resulting in the light scratch marks on the tubes aft of the aft support plate.

A total of 34 starts and 32.7-hours of thermal cycling operation at elevated temperatures with exhaust gas were accumulated on the test section. These totals include all high temperature operating periods such as heat transfer performance and structural testing as well as pretest checkout of the setup.

#### Vibration Scan

The vibration scan was carried out at room temperature with no air or gas flow through the unit. The vibratory input was as shown on Figure 2-1. The effect of temperature will be small, and will be to lower the Young's modulus of the material, resulting in a reduction of the resonant frequencies proportional to the square root of the ratio of hot and cold Young's moduli. For a type 347 stainless steel at a temperature of 1000°F, the room temperature frequency will be reduced by approximately 10 per cent. Any tube excitation due to vortex shedding by the gas flow was not simulated by this test. The vibration test results are representative only of the tube and tube bundle modes of the complete unit. It does not simulate the overall unit as regards the supporting structure modes. The structural modes can only be demonstrated by a vibration test on a complete annular unit with representative structure and mounting interface.

The test unit was assumed to be at the bottom of a complete annulus and was vibrated in the lateral and longitudinal directions, as shown on Figures 5-3 and 5-4. This position gives the most severe lateral vibratory input to the tube U-bends. The major resonant frequencies and mode descriptions are listed:

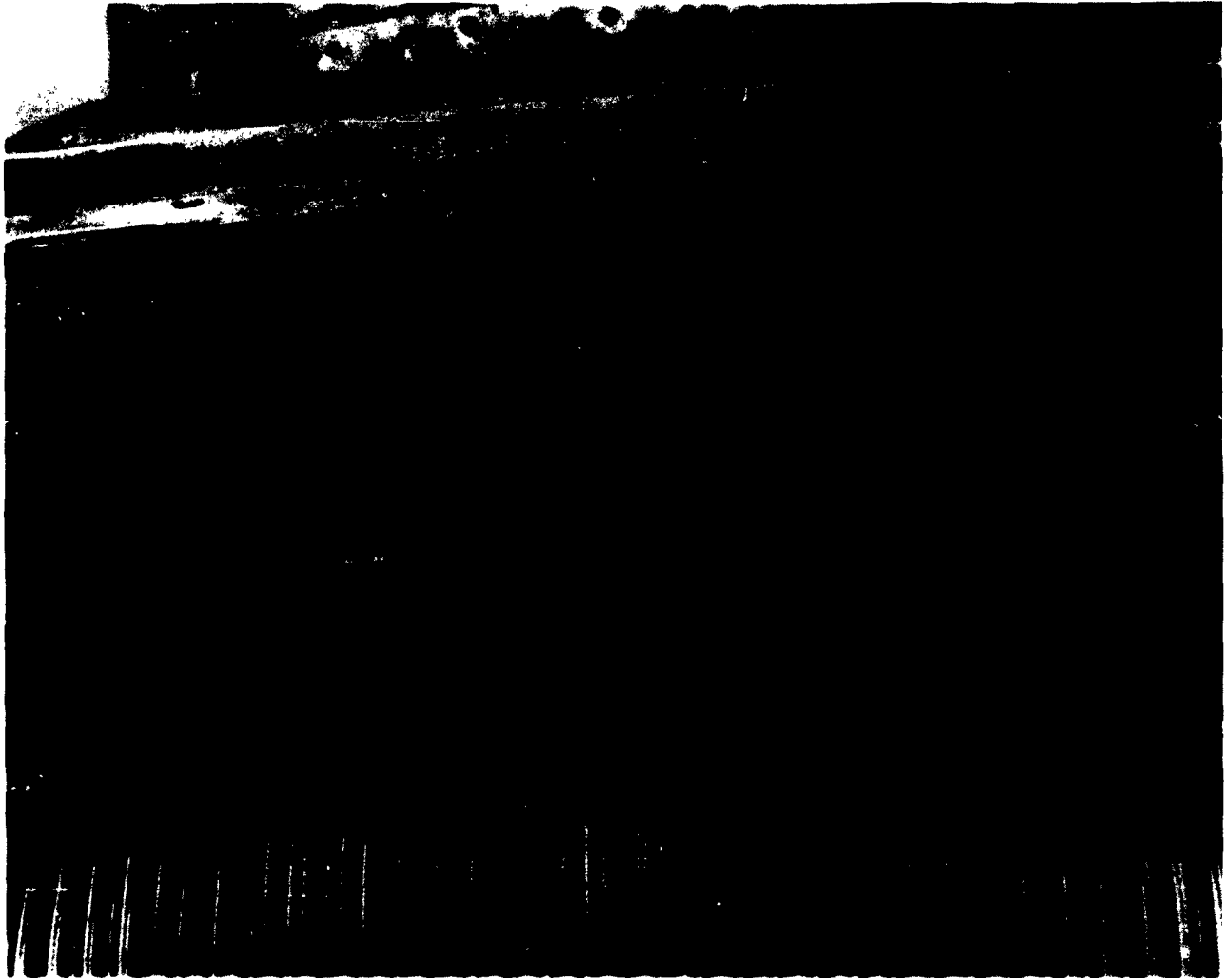


FIGURE 5-2  
TUBE SCRATCHES FROM DIFFERENTIAL EXPANSION  
RECUPERATOR ASSEMBLY 178123



FIGURE 5-3  
LATERAL VIBRATION  
RECUPERATOR ASSEMBLY 178123





FIGURE 5-4  
LONGITUDINAL VIBRATION  
RECUPERATOR ASSEMBLY 178123

#### Lateral Drive (Figure 5-3)

- \*120 cps Outside of first U-bend, lateral motion resulted.
- \*158 cps Out-of-phase motion of tube bundle sections between toroidal tube sheets and central support plate resulted. The response at the center of the tube bundle sections was approximately 4:1.
- 167 cps Third U-bend resonance occurred.
- 180 cps Lateral motion of the forward tube bundle section resulted. The aft tube bundle section had a slight elliptical motion. Response of 7:1 on the forward bundle section resulted. Fifth U-bend resonance occurred.
- \*203 cps In-phase motion of the tube bundle sections resulted. Response as high as 16:1 on the forward bundle section resulted.
- 210 cps Seventh U-bend resonance occurred.
- \*253 cps Yawing motion of the outlet duct and outlet toroid occurred. Response of 20:1 on the outlet duct flange resulted. This mode may not be representative of the final configuration.
- 292 cps Lateral motion of the outlet duct resulted. This is representative of the final configuration if bellows are used.
- 300 cps Ninth U-bend resonance occurred.

#### Longitudinal Drive (Figure 5-4)

- \*115 cps Longitudinal core excursion resulted and was reacted by supports which were attached to outlet toroidal manifold. A response of 10:1 was noted. This mode indicated the necessity for supporting the outlet toroid for longitudinal loading.
  - \*169 cps An out-of-phase tube bundle mode resulted. Vertical motion of the forward tube bundle section and circular motion of the aft tube bundle section resulted. Response of 10:1 on the aft tube bundle section was recorded.
- \* Synchronized movies were taken of these frequencies and are on file at the AiResearch Manufacturing Company.

352 cps An inlet duct vertical motion resulted which could be representative of the complete unit if bellows are used at the inlet duct connections.

During vibration scanning, the tube bundle vibration modes had displaced the central and aft support plates about 0.2 in. at the gas inlet side, as shown by Figure 5-5. The support plates were not attached to and held in place by the exhaust gas outlet manifold during this test, and were free to slide on the tubes in this area. The vibration characteristics were attenuated by the lack of support imposed by the test unit design, which represented only one-sixth of a full annulus. It was evident that incorporation of plate attachments along with intrinsic stability of the full core would result in a design free of destructive vibration.

It is estimated that the stress level in the tubes during the tube bundle modes is approximately 5000 psi. The fundamental mode of the tube between the spacer plates, which occurs around 2500 cps, was not excited, as this frequency lies above the specified frequency range for this test.

#### Static U-Tube Bend Tests

Static bend tests have been carried out on U-tubes with different radii to compare their longitudinal flexibility with calculated values and to establish their capacity to absorb differential thermal growth between the two straight sections of the U-tube. The test fixture simulated differential thermal expansion by fixing one leg of the U-tube and loading the other. The tube was supported at intervals which simulated the support obtained by the spacer and support plates in the unit.

The test data indicated that, for the smaller radius tubes, the longitudinal stiffness was between 64 and 77 per cent of the calculated value without flexibility factors. For these tubes, crippling occurred on the inside of the U-bend near the first support on the fixed leg at a load value above the yield load. The calculated yield values appeared fairly consistent with the test data, although on some tubes, a slight permanent set occurred before the calculated yield load was reached. Measured stiffness of the large radius U-tubes agreed almost exactly with the calculated values without flexibility factors. The smaller radii U-bends had more tube

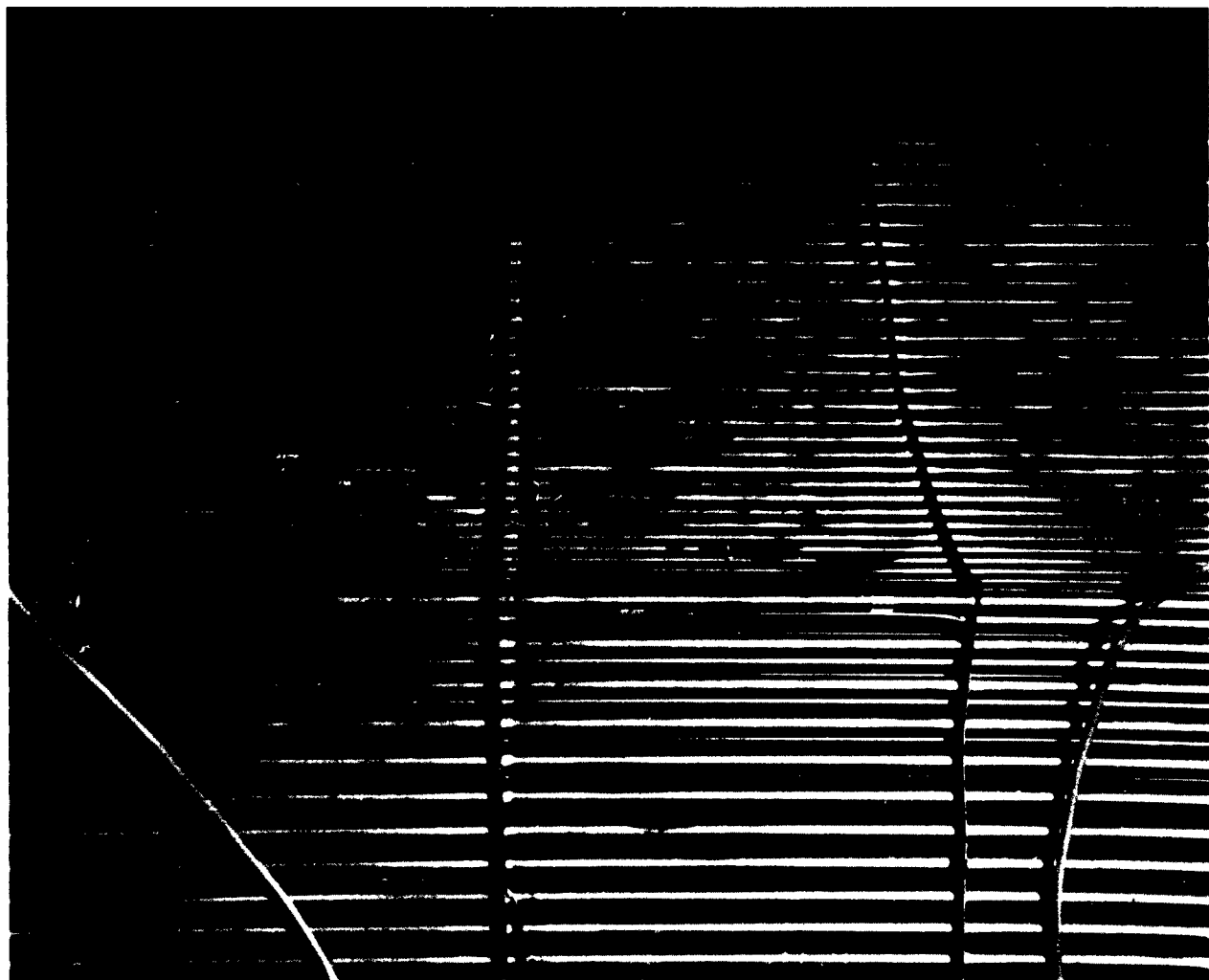


FIGURE 5-5  
CENTER SUPPORT PLATE SHIFT  
RECUPERATOR ASSEMBLY 178123

cross-section ovality than the larger radii bends, which may be one reason for their increased flexibility.

On the basis of this data, the minimum U-tube mean bend radius should be increased from the present value of 1.1 in. to 1.60 in. to absorb the transient differential expansion, as discussed in the section on Temperature Measurements - Steady-State and Transient. The outer U-bends have sufficient margin to absorb the transient without increase in radius.

#### "Stresscoat" Test

A "Stresscoat" brittle lacquer test has been conducted on the toroidal manifolds and inlet and outlet ducting. Test results are shown on Figure 5-6. The test was made at room temperature and the pressure raised in increments to a pressure of 590 psig, which is equivalent to the proof condition of 229 psig at 942°F. Analysis of the stress distribution and intensity may influence the selection of the thickness of the toroidal manifolds and associated ducting for the complete unit. It is possible that the gauge of the forward halves of the toroidal manifolds can be reduced, and the reinforcing in the area of the air inlet duct can be modified. Tie rods should be incorporated at the trailing edges of the internal support webs in the inlet duct. Tie rods with a doubler along the duct-toroid junction will reduce the stress concentration at the weld of the inlet duct to the toroidal manifold.

#### Leakage

After completion of fabrication and assembly, but before testing, air pressure of 185 psig at room temperature was applied to the tube side of the recuperator. Zero leakage resulted. After completion of all tests, including heat transfer, temperature measurements and vibration, air pressure of 185 psig at room temperature was again applied and leakage was 0.0000222 lb per sec. This value is essentially zero.

RECUPERATOR ASSEMBLY X178175 (EIT)

#### Temperature Measurements - Steady-State and Transient

The purpose of these temperature measurements was first, to confirm calculated steady-state temperature distribution, and second, to investigate the possibility of transient conditions that might influence the design

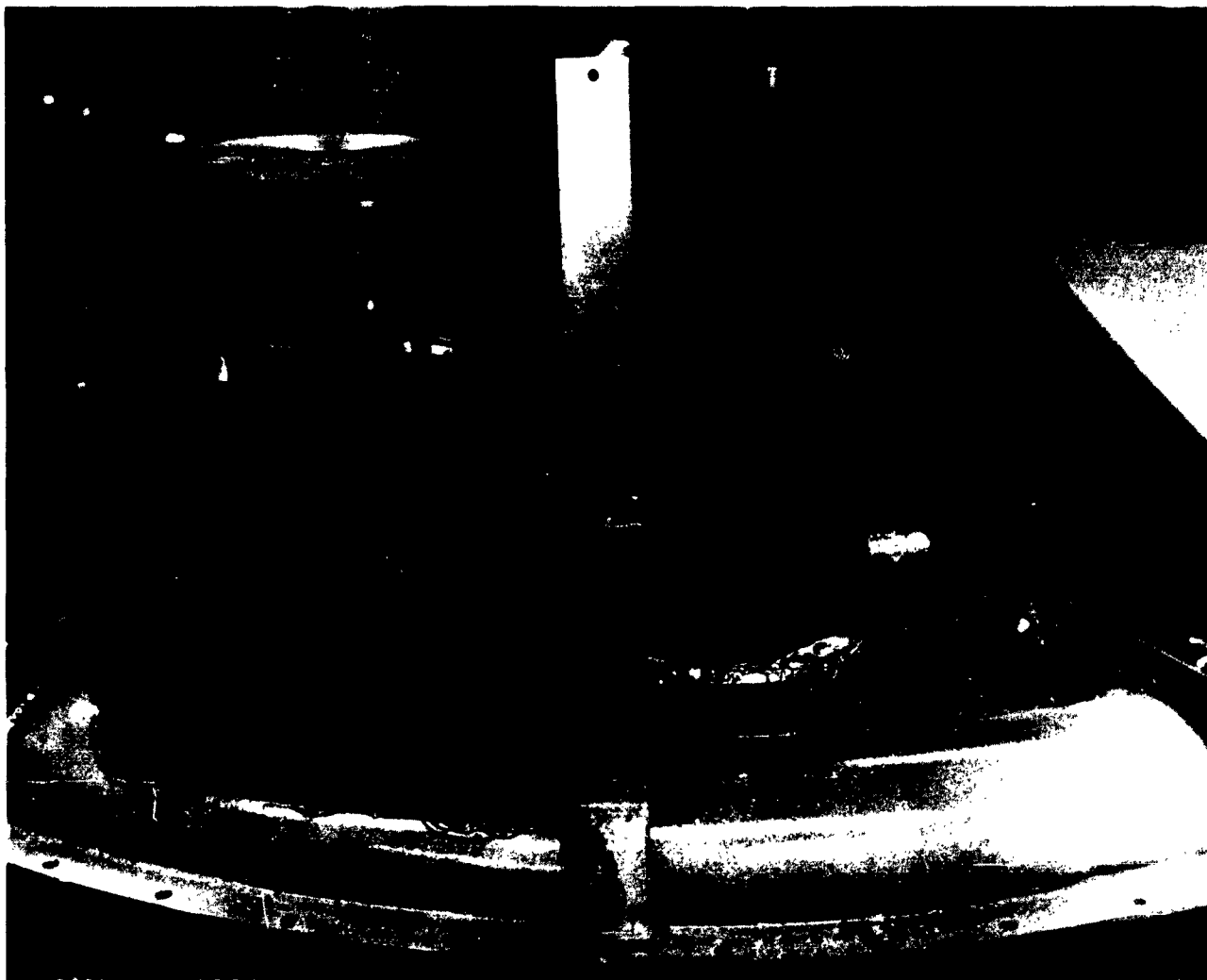


FIGURE 5-6  
STRESSCOAT PATTERNS  
RECUPERATOR ASSEMBLY 178123

philosophy. The most critical steady-state condition is represented by values shown on Table 2-2. The most severe transients will probably be experienced during start to cruise. The transient input was based upon conditions shown on Figure 2-2.

There is an approximate agreement between the theoretical and measured temperature distributions, even though previously noted uncertainties exist about accurately measuring true mean metal temperatures.

The measured steady-state tube temperatures show that the mean metal temperature for any tube in the core is approximately the same. The mean metal temperature of the tube adjacent to the air inlet and outlet face is somewhat lower than the other tubes in the core due to a small amount of bypass air which cooled the section of the tube at the air outlet. The steady-state plate temperatures and temperature gradients differed somewhat from design point values because of the bypassing air. Typical curves of temperature and pressure variations with time for start to cruise are shown in Figure 5-7.

Analysis of the transient temperatures indicates very little lag in the tube temperature which, if present, would cause transient differential tube expansion and loading of the tube sheets and tubes. The tubes at the outside diameter of the bundle will have the largest temperature differential. The tubes in the area of the cooling air inlet face cool faster than other tubes when the air is introduced; however, with no air bypassing, this should be offset by these same tubes cooling slower than other tubes in the air outlet area. Analysis of the test data shows that no transient temperature gradients greater than the steady-state conditions appeared to exist in the tube sheets or support plates.

A total of 21 starts and 40.4 hours of thermal cycling operation at elevated temperatures with exhaust gas, plus 16.6 hours at ambient temperatures were accumulated on the test section. These totals include all operating periods, such as heat transfer performance and structural testing, as well as pretesting checkout of the setup.

#### Vibration Scan

The vibration scan was carried out at room temperature with no air or gas flow through the unit. As shown by Figure 5-8 and 5-9, the vibratory





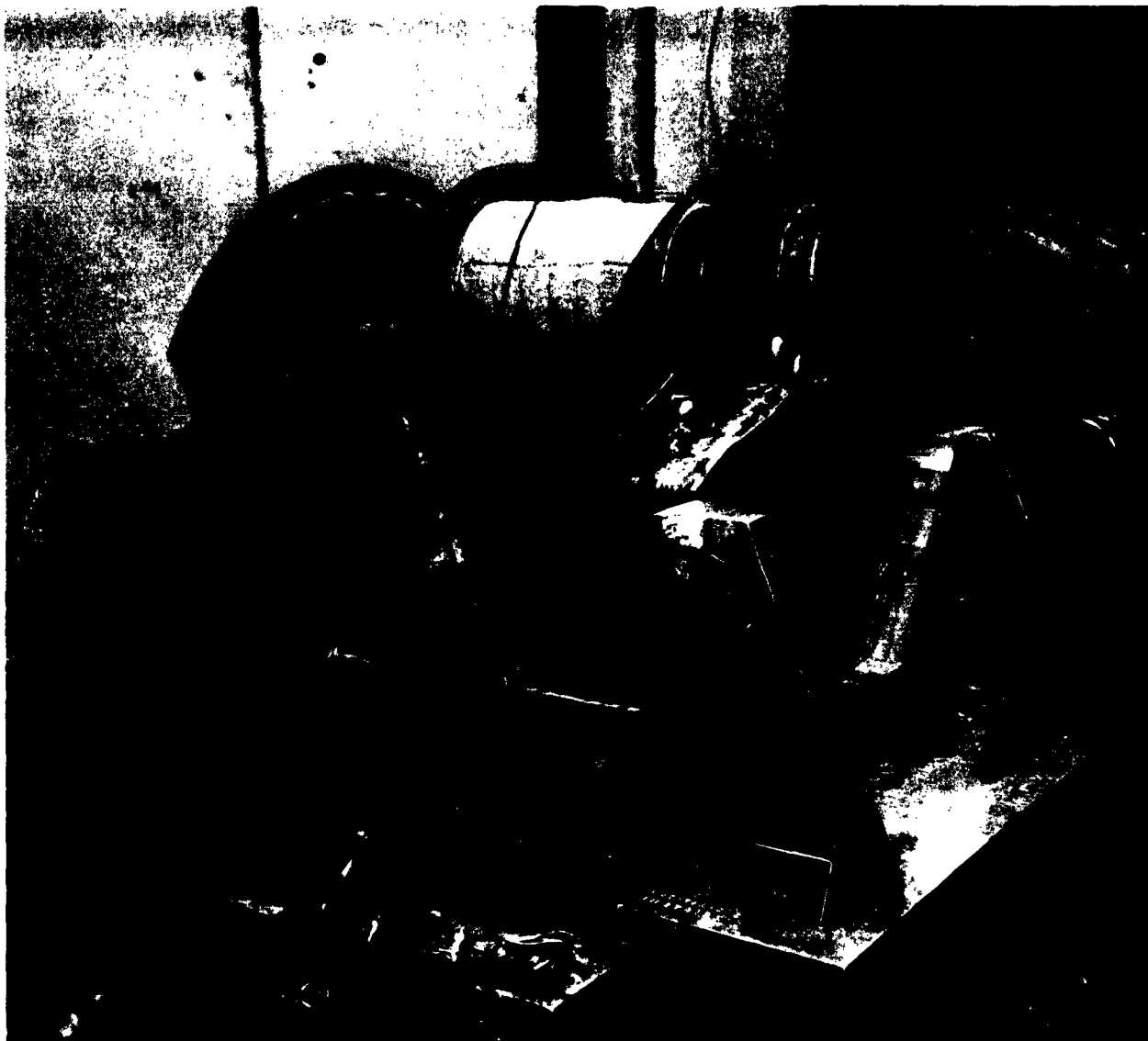


FIGURE 5-8  
LATERAL VIBRATION  
RECUPERATOR ASSEMBLY X178175

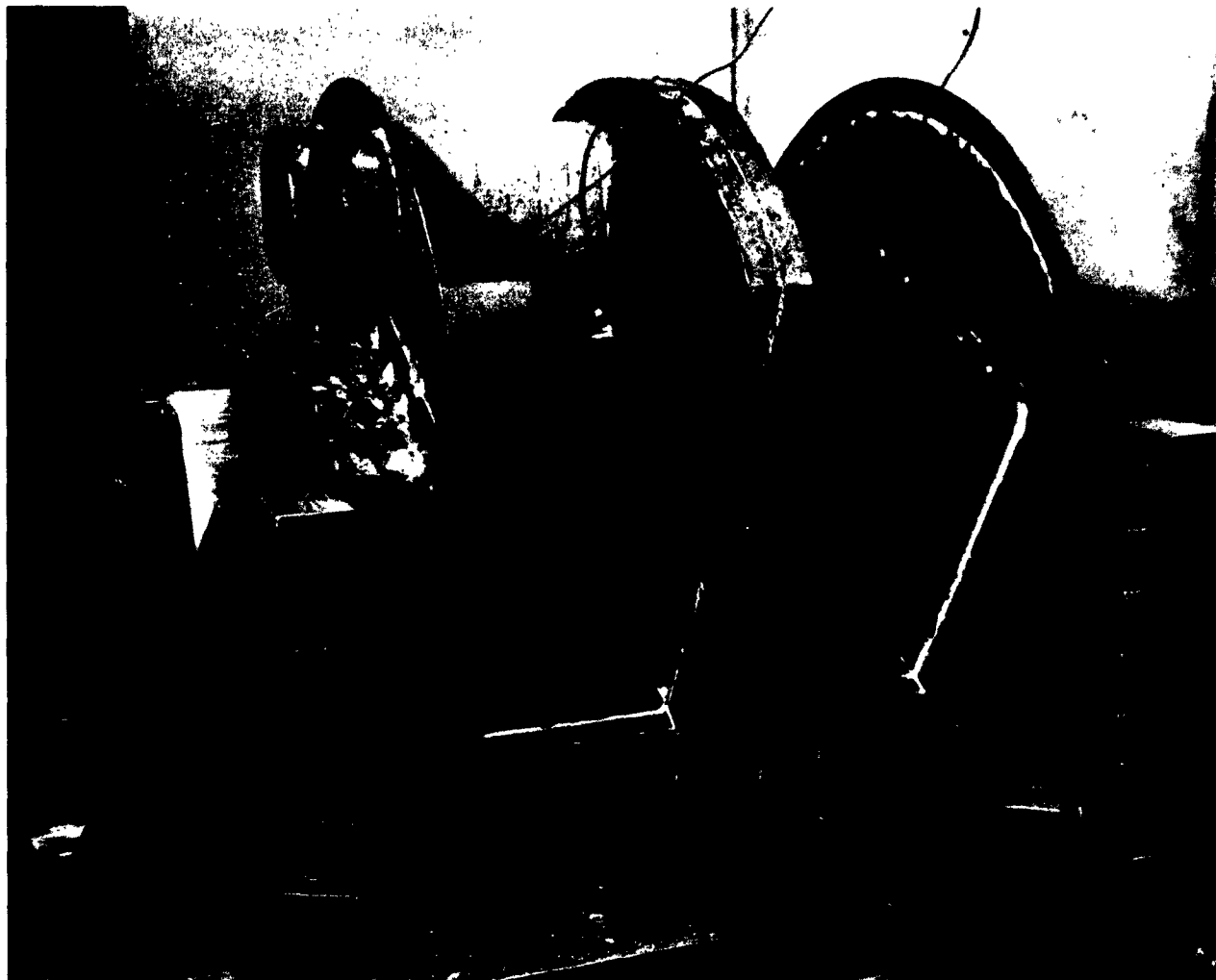


FIGURE 5-9  
LONGITUDINAL VIBRATION  
RECUPERATOR ASSEMBLY X178175

Input and drive planes were identical to those used for the (EOT) test section. The effect of temperature will be to slightly reduce the value of the resonant frequencies as described in the section about (EOT) vibration scan. This vibration test is limited to demonstrating the tube bundle modes alone, and it is not representative of structural modes or aerodynamic tube excitation.

The vibration fixture used did not provide radial support at the central baffle plate and, in this respect, is not representative of the complete unit. The modes which are not representative will be indicated in the following tabulation.

Lateral Drive (Figure 5-8)

- \*109 cps Fundamental motion of the complete tube bundle between the tube sheets occurred. The response measured on the central baffle plate was approximately 15:1. This mode is not representative of the final design, as there will be radial support at the center of the tube bundle.
- 248 cps In-phase motion of the tube bundle section on either side of the central support plate resulted. A response of 3:1 was measured on the aft spacer plate.
- 340 cps Motion similar to the 248 cps mode with a response of approximately 7:1 occurred.
- \*356 cps Out-of-phase motion of the tube bundle sections resulted. Aft spacer plate response was 13:1.
- 450 cps Motion of tubes in the area of the central baffle plate resulted.

Longitudinal Drive (Figure 5-9)

- 37 cps Resonance of the overhung area of the central baffle plate resulted. This is not representative of the final unit.

\* Synchronized movies were taken of these frequencies and are on file at the AResearch Manufacturing Company.

- 101 cps A 2:1 response normal to the tubes near the central baffle plate resulted. Resonance of the overhung area of the forward tube sheet driving the tube bundle resulted. This mode is not representative of the final design.
- 213 cps Motion similar to that at 101 cps occurs with 4:1 response. This looks like the first harmonic of the forward tube sheet.
- 305 cps Resonance of the overhung area of the aft support plate occurred. This mode is not representative of the final design.
- 460 cps An 8:1 response occurred at the accelerometer mounted normal to the tubes near the central baffle plate. This could be a higher harmonic of the tube bundle between the tube sheets. It was possible to slide the central baffle plate on the tubes during this resonance.

After scanning, it was noted that the spacer plates had moved as much as 0.25 in. on the tubes at the internal radius. There were no resonances of any concern in the longitudinal axis except at 460 cps, which also appeared in the lateral axis. Since adequate support against longitudinal tube bundle motion was provided by angles attached to 0.25-in. thick transition ducts on the tube sheet, no longitudinal core motion was observed. The final design must also incorporate longitudinal support for the tube bundle, possibly with radial gussets to the outer shell at the aft tube sheet.

#### Tube Collapsing Test

Since the (EIT) recuperator contains the high pressure fluid outside tubes, tests were conducted on sample tubes to determine the amount of external pressure required to cause collapsing. The samples were cut to length, brazed to tube sheets, and assembled inside a test fixture that permitted application of external pressure hydrostatically at room temperature. The average collapsing pressure was found to be 750 psig. Based on material properties at room temperature and operating temperature, 750 psig is equivalent to 570 psig at a temperature of 1050°F. This represents a margin of safety of 2.85 to 1 over the maximum design operating pressure.

The predicted collapsing pressure obtained from equations given in standard references was 497 psig. The higher test value obtained was due

primarily to departures from theory in tube-diameter-to-wall-thickness ratio, and tube configuration selections. A lack of data in the literature required these empirical measurements on the tubes. Based on the tests conducted, no problem is expected regarding tube collapsing. However, concurrent with the start of design in Phase II, tests will be run on additional samples at room temperature and at design temperature in order to establish further control data.

#### Leakage

After completion of fabrication and assembly, but before testing, air pressure of 15 psig at room temperature was applied to the tube side of the recuperator. Zero leakage resulted. After completion of tests, including heat transfer, temperature measurement and vibration, air pressure of 15 psig at room temperature was again applied to the tube side and the leakage rate was 0.00163 lb. per sec. This is an extremely low rate, similar to the (EOT) value, but higher than would normally be expected since the test section was disassembled and modified four times in the course of testing to accomodate various test setups.

## SECTION 6

### PARAMETRIC STUDY

A parametric study was undertaken to determine the optimum recuperator for a 2700 hp class turboshaft gas turbine engine. Various heat transfer surfaces, such as plate-fin, finned tube, and bare tubes were investigated during the course of the study, as well as variations in surface geometry for the more promising surfaces. The results of this study indicate that bare tube units in a cylindrical configuration will result in near optimum solutions. Both (EIT) and (EOT) recuperators were considered in the study and the best surfaces for each were used in the 60 degrees of arc test units built during Phase I of this program.

A comparison of the relative merits of the (EIT) and (EOT) bare tube recuperators indicates that the (EIT) unit is superior with regard to thermal stress, weight, volume, reliability, producibility, maintainability, and cost.

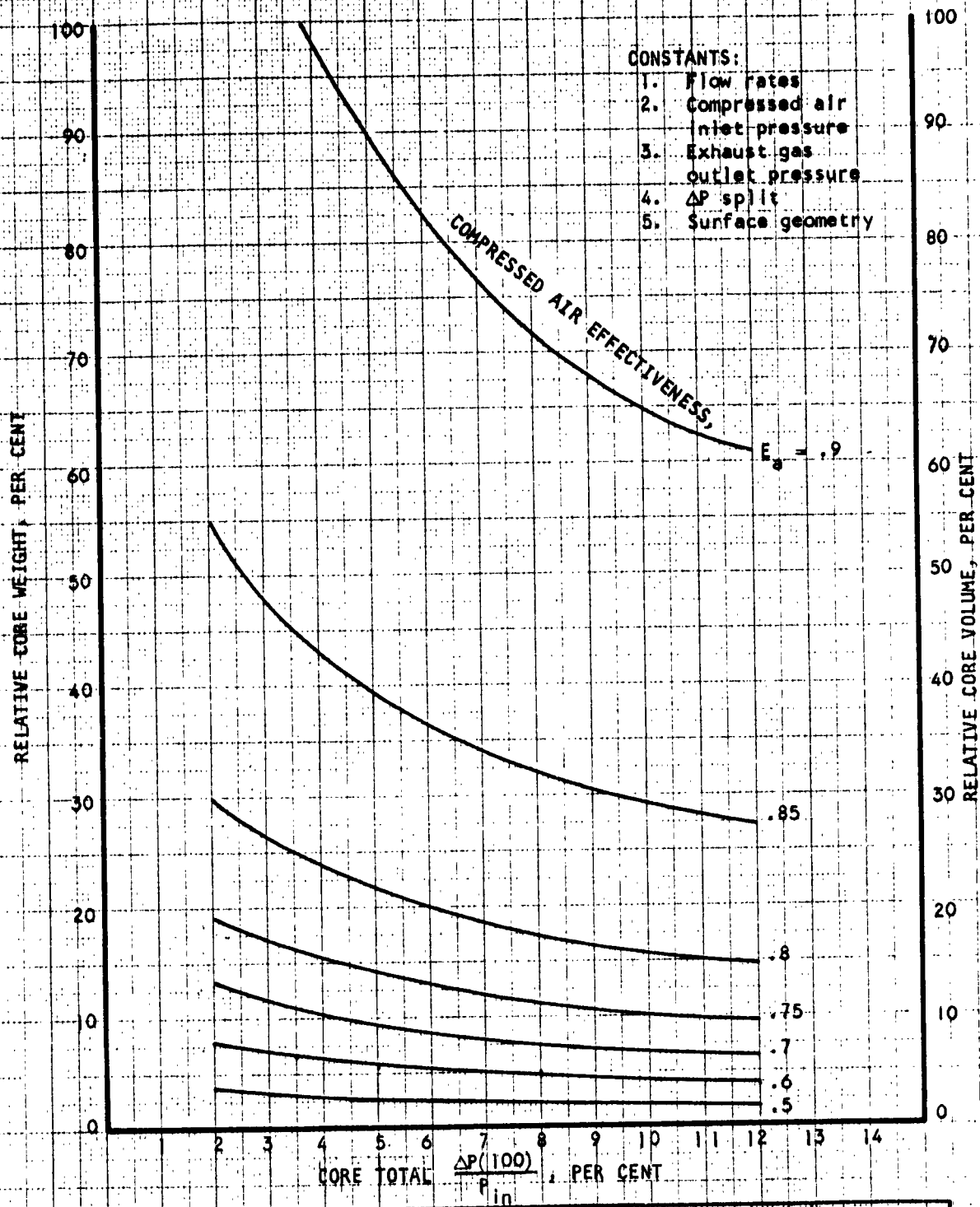
Several curves obtained during the study of the (EIT) bare tube recuperator have been selected for presentation in this section to illustrate the change in core weight and size with variations in effectiveness and/or per cent pressure drop. The trends indicated by these curves are generally applicable to any type heat transfer surface or configuration, although the shape of the curves and weight and size minimums will tend to vary from surface to surface.

Figure 6-1, which presents relative core weight versus per cent core pressure drop, with effectiveness plotted as a parameter, indicates that, at the design point operating conditions for the subject recuperator, which is at approximately 8 per cent pressure drop, an increase in core weight by a factor of approximately 2.3 is realized by going from 0.7 effectiveness to 0.8 effectiveness. This curve very dramatically illustrates the sharp increase in core weight that is realized with only slight increase in effectiveness at the higher effectiveness values. It also shows a substantial reduction in weight as the per cent pressure drop is increased at 0.9 effectiveness.

The variation in recuperator dimensions with increasing effectiveness is shown on Figure 6-2. This figure illustrates the same general trend that was noted in Figure 6-1; that is, the sharp increase in relative core dimensions or weight at the high effectiveness values. The  $L_o$  and  $L_t$  dimensions are almost asymptotic at 0.9 effectiveness. It is also interesting to note that the OD dimension decreases with increasing effectiveness, reaches a minimum, and then increases.

The effect of variations in the pressure drop split on relative core weight and dimensions at the critical design conditions is shown on Figure 6-3. Note that a split of 3 to 1 in favor of the exhaust gas side results in minimum relative core weight and a near minimum recuperator OD and tube length. The (EIT) recuperator test core was designed with this pressure drop split.

The parametric study included a consideration of weight attributable to tube sheets, tube support plates, and normal recuperator manifolding. The percentage of the overall recuperator weight allocated to these items varies with recuperator dimensions and volume. Generally speaking, however, this percentage will vary as the core volume, that is, large core volumes will have a small percentage of the overall recuperator weight attributable to these items and for small core volumes the inverse is true.



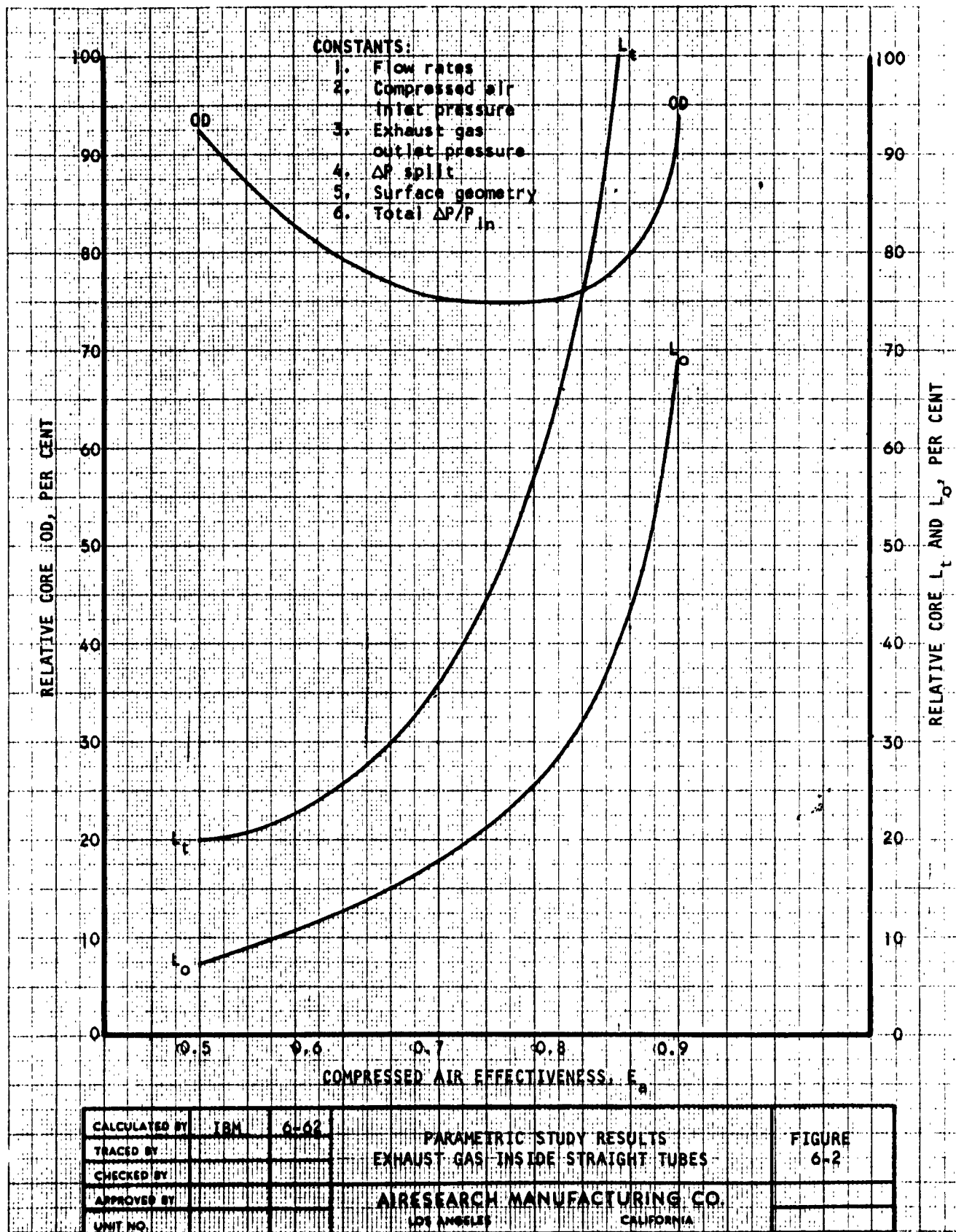
CALCULATED BY	IBM	6-62
TRACED BY		
CHECKED BY		
APPROVED BY		
UNIT NO.		

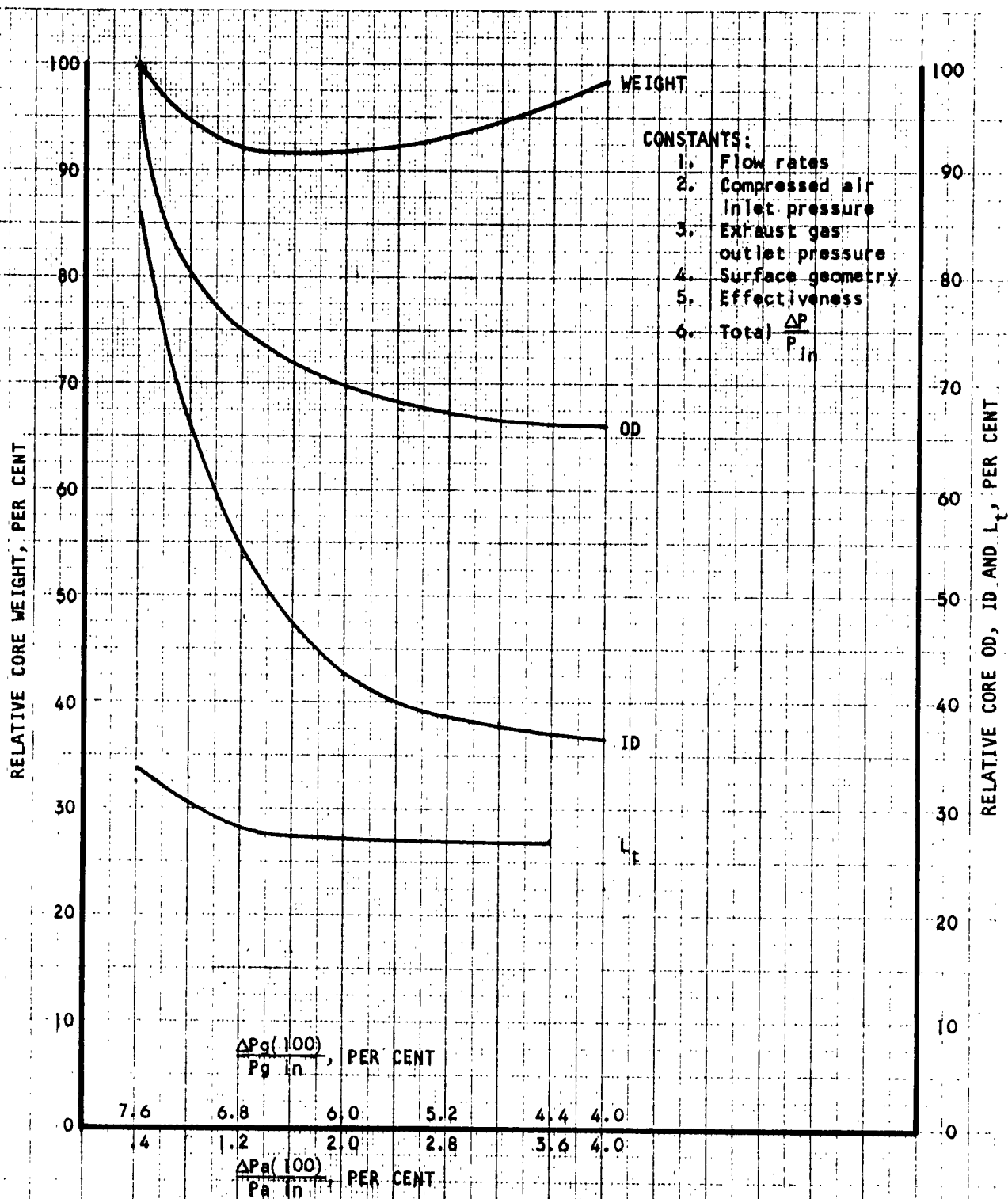
PARAMETRIC STUDY RESULTS  
EXHAUST GAS INSIDE STRAIGHT TUBES

AIRESEARCH MANUFACTURING CO.  
LOS ANGELES CALIFORNIA

FIGURE  
6-1







CALCULATED BY	IBM	7-62	PARAMETRIC STUDY RESULTS EXHAUST GAS INSIDE STRAIGHT TUBES	FIGURE 6-3
TRACED BY				
CHECKED BY			AIRESEARCH MANUFACTURING CO.	
APPROVED BY				
UNIT NO.			LOS ANGELES CALIFORNIA	

## SECTION 7

### RECUPERATOR DESIGN

This section presents a recuperator design procedure and surface performance characteristics to enable the designer to obtain recuperator size and weight at specific design conditions. In designing a recuperator for a specific engine application, the designer will be limited to a minimum recuperator ID and maximum practical OD and tube length. Within these bounds, there will undoubtedly be several designs which will meet a given problem statement. It will be up to the designer's discretion to select the best solution for his application considering such factors as size, weight, mounting provisions, and vibration characteristics.

As a result of optimization studies on recuperators of this type, it has been determined that a two pass cross counterflow configuration is near optimum. Therefore, the design procedure outlined in this section is for this configuration only. Performance curves for designing both (EIT) and (EOT) recuperators are included herein. Generally speaking (EIT) recuperator designs will be lighter, have larger OD and shorter tube length than (EOT) recuperator designs. A separate and distinct design procedure is outlined below for each type recuperator. Symbols and terms used in the procedures are defined in the nomenclature.

#### CALCULATION PROCEDURE (EIT) RECUPERATOR

1. Select critical operating condition for recuperator design.
2. Calculate effectiveness for both sides of recuperator.

$$E_{\text{hot}} = \frac{\Delta T_{\text{hot}}}{T_{\text{hot in}} - T_{\text{cold in}}}$$

$$E_{\text{cold}} = \frac{\Delta T_{\text{cold}}}{T_{\text{hot in}} - T_{\text{cold in}}}$$

3. Calculate minimum capacity rate ratio which is between 0 and 1.

$$\frac{WC_{\text{hot}}}{WC_{\text{cold}}} \text{ or } \frac{WC_{\text{cold}}}{WC_{\text{hot}}}$$

4. Read number of transfer units required from Figure 7-2 with minimum capacity rate ratio and effectiveness of side that has minimum capacity rate.

5. Calculate required UA.

$$\text{Required UA} = (\text{NTU}) (\text{WC}) \min$$

6. Calculate required corrected air pressure drop.

$$\sigma \Delta P_a = \left( \frac{P}{0.0765} \right) (\Delta P)$$

7. Calculate required corrected exhaust gas pressure drop.

$$\sigma \Delta P_g = \left( \frac{P}{0.0765} \right) (\Delta P)$$

8. Assume recuperator OD, ID, and tube length dimensions consistent with application requirements.

9. Calculate flow per square foot of frontal area on both sides of recuperator.

$$\frac{W_i}{A_i} = \frac{576 W_i}{\pi (OD)^2 - \pi (ID)^2}$$

$$\frac{W_o}{A_o} = \frac{288 W_o}{(L_n)(L_t)}$$

10. Read  $\frac{UA}{V}$  from Figure 7-3.

11. Calculate available UA.

$$\text{Available UA} = \frac{UA}{V} \left( \frac{L_o L_t L_n}{1728} \right)$$

12. Read  $\frac{\sigma \Delta P_i}{L_t}$  from Figure 7-4.

13. Calculate available  $\sigma \Delta P_i$ .

$$\text{Available } \sigma \Delta P_i = \left( \frac{\sigma \Delta P_i}{L_t} \right) (L_t)$$

14. Read  $\frac{\sigma \Delta P_o}{L_o}$  from Figure 7-4.

15. Calculate available  $\sigma\Delta P_o = \left(\frac{\sigma\Delta P_o}{L_o}\right) (L_o)$

16. Available values of UA,  $\sigma\Delta P_i$  and  $\sigma\Delta P_o$  must agree with required values or the assumed recuperator dimensions must be varied and steps 9 through 15 repeated until a balance is obtained. An increase in  $L_n$  while maintaining  $L_o$  and  $L_t$  will result in lower pressure drops on both sides. Conversely a reduction in  $L_n$  while maintaining the other two dimensions will result in higher pressure drops on both sides. Increases or decreases in UA values are proportional to core volume changes.

17. Calculate recuperator tube bundle weight.

$$\text{Tube bundle weight} = 0.0141 (L_o L_t L_n), \text{lb}$$

18. Calculate overall recuperator weight.

$$\text{Overall recuperator weight} = 1.75 \text{ tube bundle weight}$$

This value includes the weight of normal manifolding as well as tube sheets and tube support structure but does not include any weight attributable to mounting. Also, the factor used to obtain overall weight from core weight is specific for the class of engine being considered in this program. Larger engines will require larger recuperators which will have a lower factor whereas for smaller engines the reverse will be true.

Overall recuperator dimensions will vary depending upon the specific application. Allowance must be made for manifolding on both sides of the recuperator. Sufficient free flow area should be provided in the manifolding to reduce parasitic pressure drop to a minimum.

#### CALCULATION PROCEDURE (EOT) RECUPERATORS

1. The first seven steps of the calculation procedure for (EIT) recuperators outlined above should be followed as stated. These calculations pertain only to the required performance of the recuperator and do not pertain to any specific recuperator surface.

2. Assume recuperator OD, ID, and tube length dimensions consistent with application requirements.
3. Calculate flow per square foot of frontal area on both sides of recuperator.

$$\frac{W_i}{A_i} = \frac{1152 W_i}{\pi(OD)^2 - \pi(ID)^2}$$

$$\frac{W_o}{A_o} = \frac{144 W_o}{(L_n)(L_t)}$$

4. Read  $\frac{UA}{V}$  from Figure 7-5.

5. Calculate available UA.

$$\text{Available UA} = \frac{UA}{V} \left( \frac{L_o L_t L_n}{1728} \right)$$

6. Read  $\frac{\sigma \Delta P_i}{L_t}$  from Figure 7-6

7. Calculate available  $\sigma \Delta P_i$ .

$$\text{Available } \sigma \Delta P_i = \left( \frac{\sigma \Delta P_i}{L_t} \right) (L_t)$$

8. Read  $\frac{\sigma \Delta P_o}{L_o}$  from Figure 7-6

9. Calculate available  $\sigma \Delta P_o$ .

$$\text{Available } \sigma \Delta P_o = \left( \frac{\sigma \Delta P_o}{L_o} \right) (L_o)$$

10. Available values of UA,  $\sigma \Delta P_i$  and  $\sigma \Delta P_o$  again must agree with required values or new recuperator dimensions must be assumed and steps 3 through 9 repeated until balance is obtained.

11. Calculate recuperator tube bundle weight.

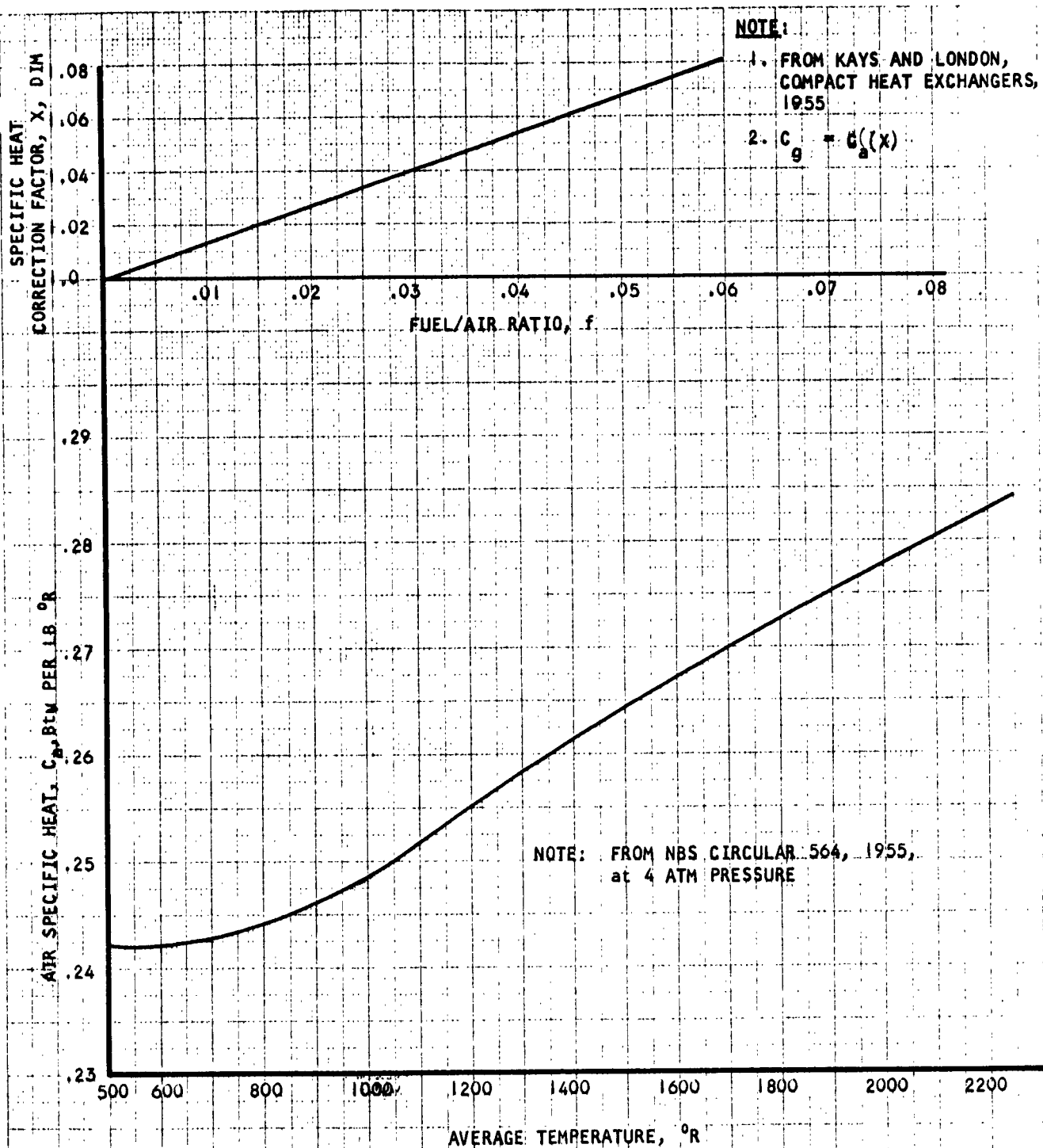
$$\text{Tube bundle weight} = 0.0153 (L_o L_t L_n), \text{lb}$$

12. Calculate recuperator weight.

$$\text{Recuperator weight} = 2.0 \text{ tube bundle weight}$$

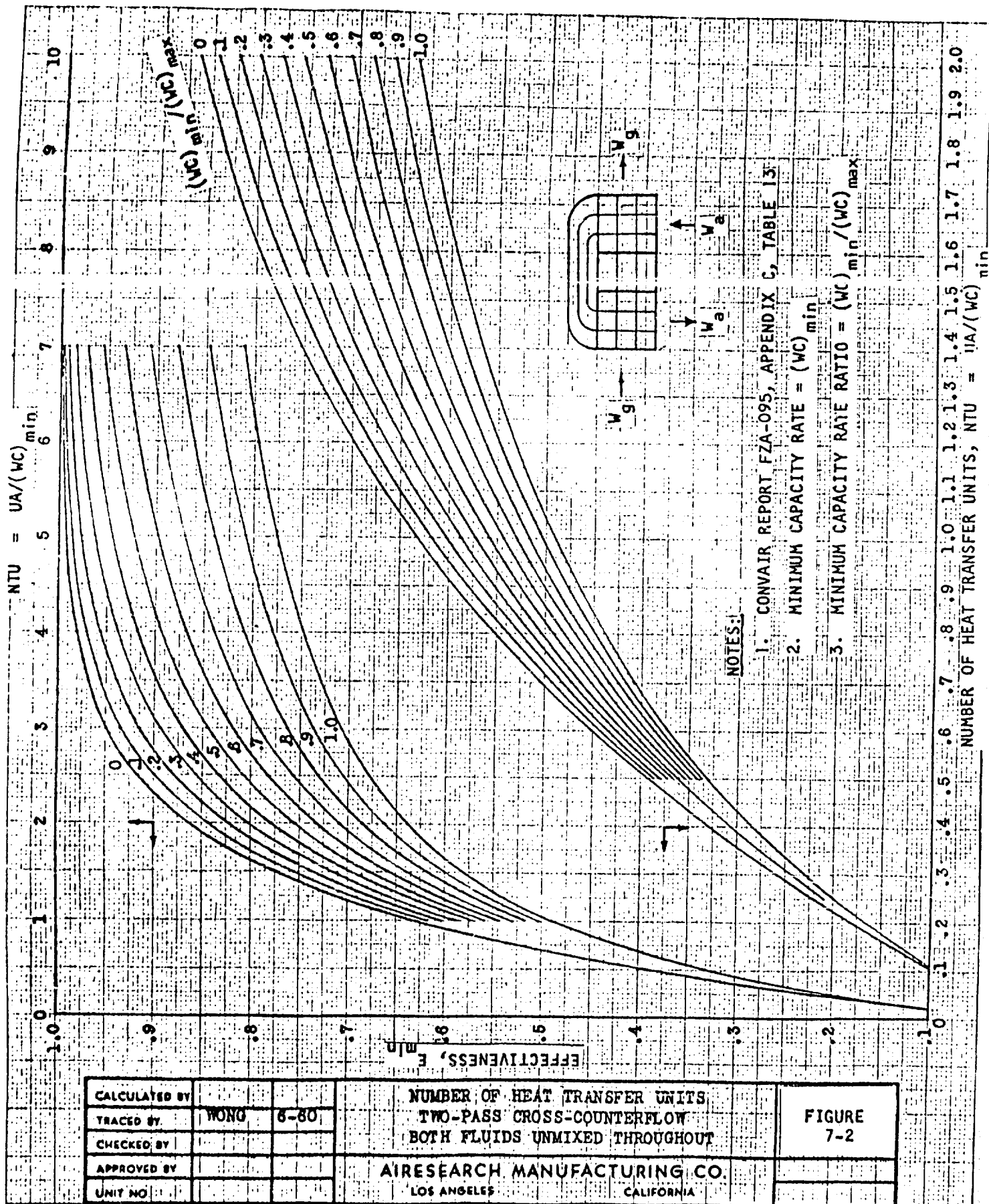
The comments regarding recuperator weight and overall dimensions stated under the (EIT) recuperator design procedure apply as well to the (EOT) recuperator. However, an additional allowance must be made for interpass space on the (EOT) recuperator. An increase of approximately 2.0 inches in recuperator OD and a corresponding decrease in recuperator ID will be required.

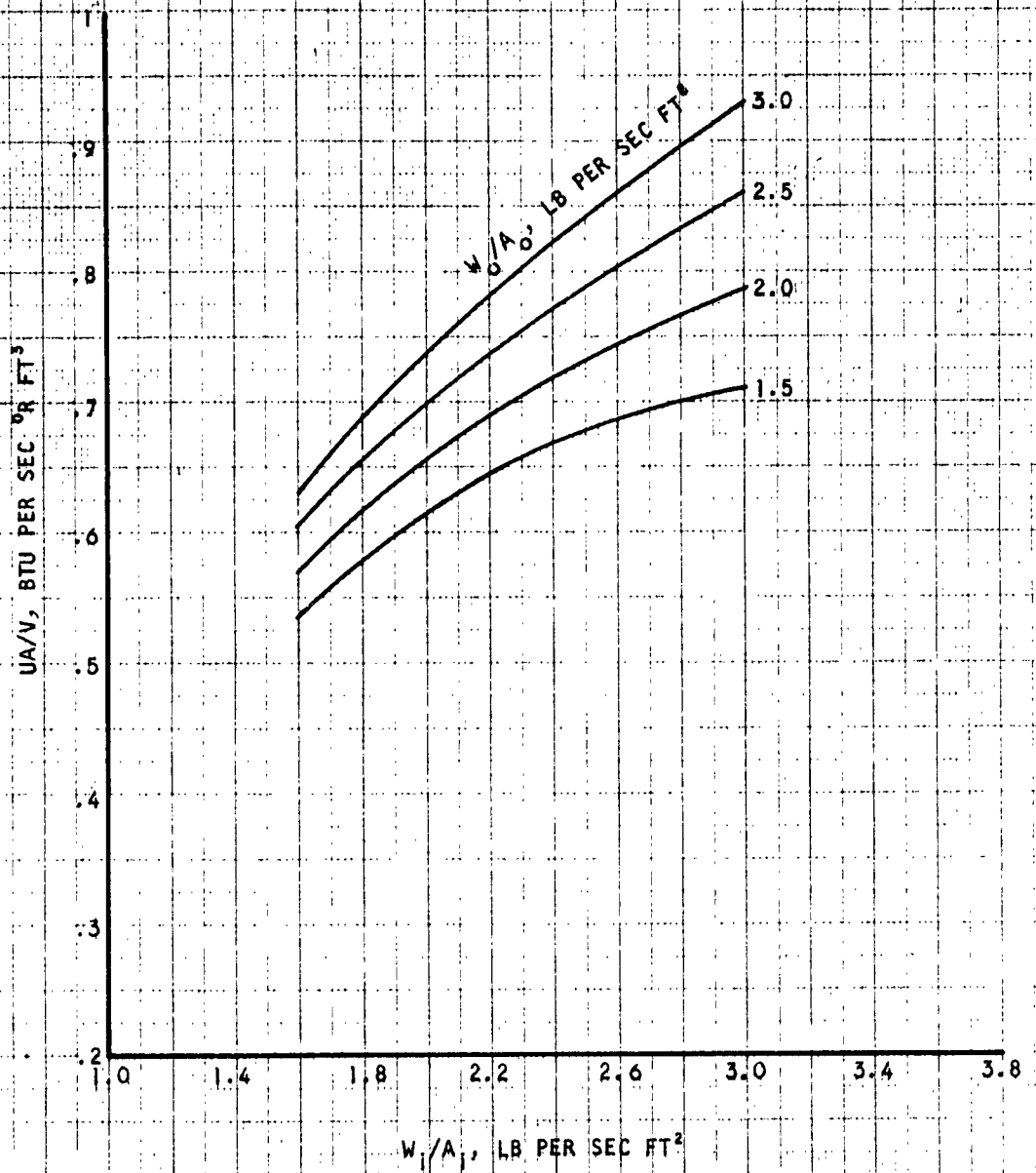
The design procedures and performance parameters presented in this section can be used by the engine or airframe manufacturer to conduct an optimization study to obtain a near optimum recuperator for a specific application. The two surfaces presented herein were selected as best for the class of engine being covered in this program as a result of a parametric study which investigated various types of heat transfer surfaces as well as various modifications of surface geometry for a specific type of heat transfer surface. The designer should refer to the curves in Section 6, Parametric Study, which will serve as a guide in the selection of new recuperator core dimensions after the initial calculation has been performed.



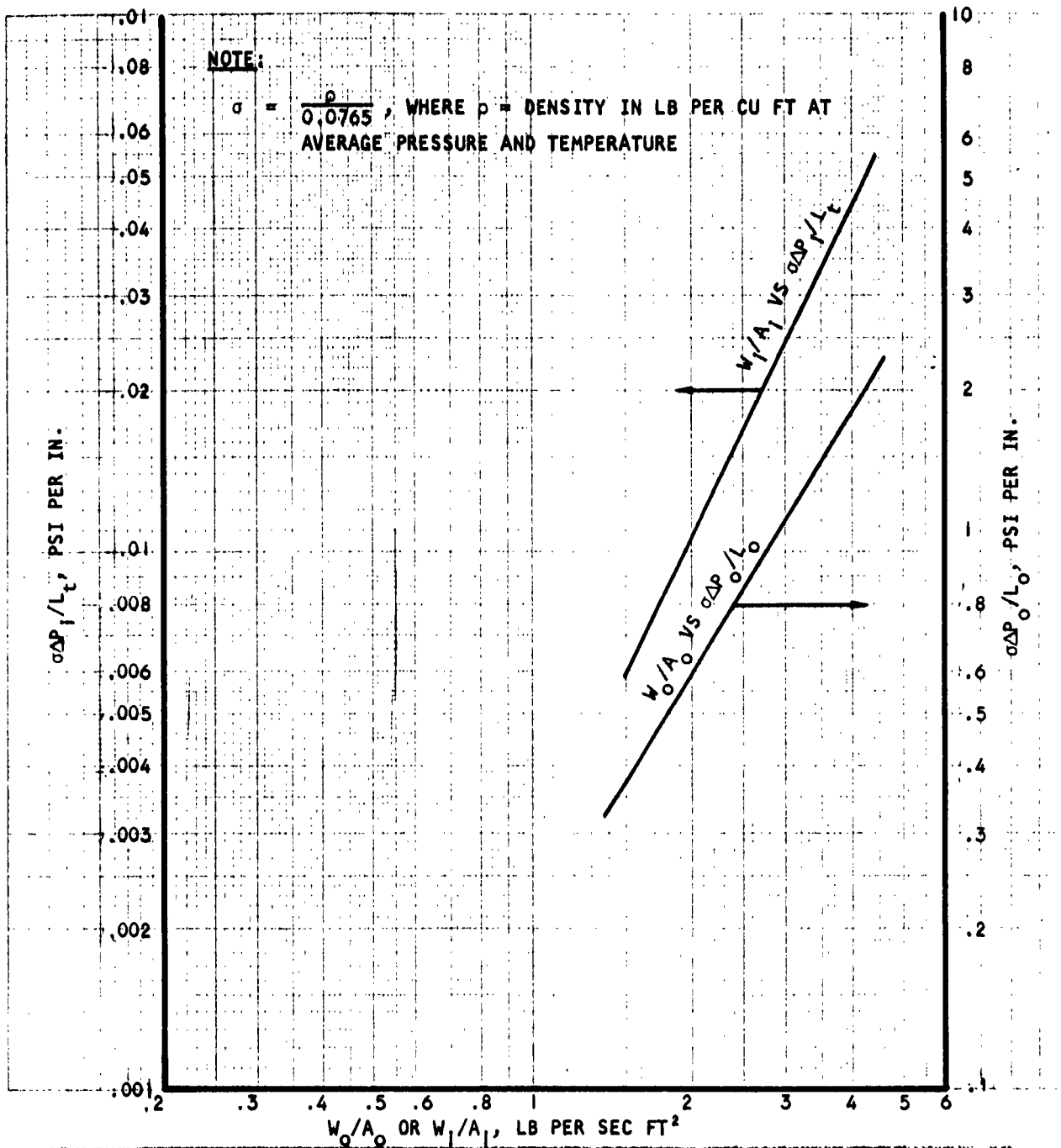
CALCULATED BY		8-62	AIR AND EXHAUST GAS SPECIFIC HEAT	FIGURE 7-1
TRACED BY				
CHECKED BY				
APPROVED BY				
UNIT NO.			AIRESEARCH MANUFACTURING CO. LOS ANGELES CALIFORNIA	



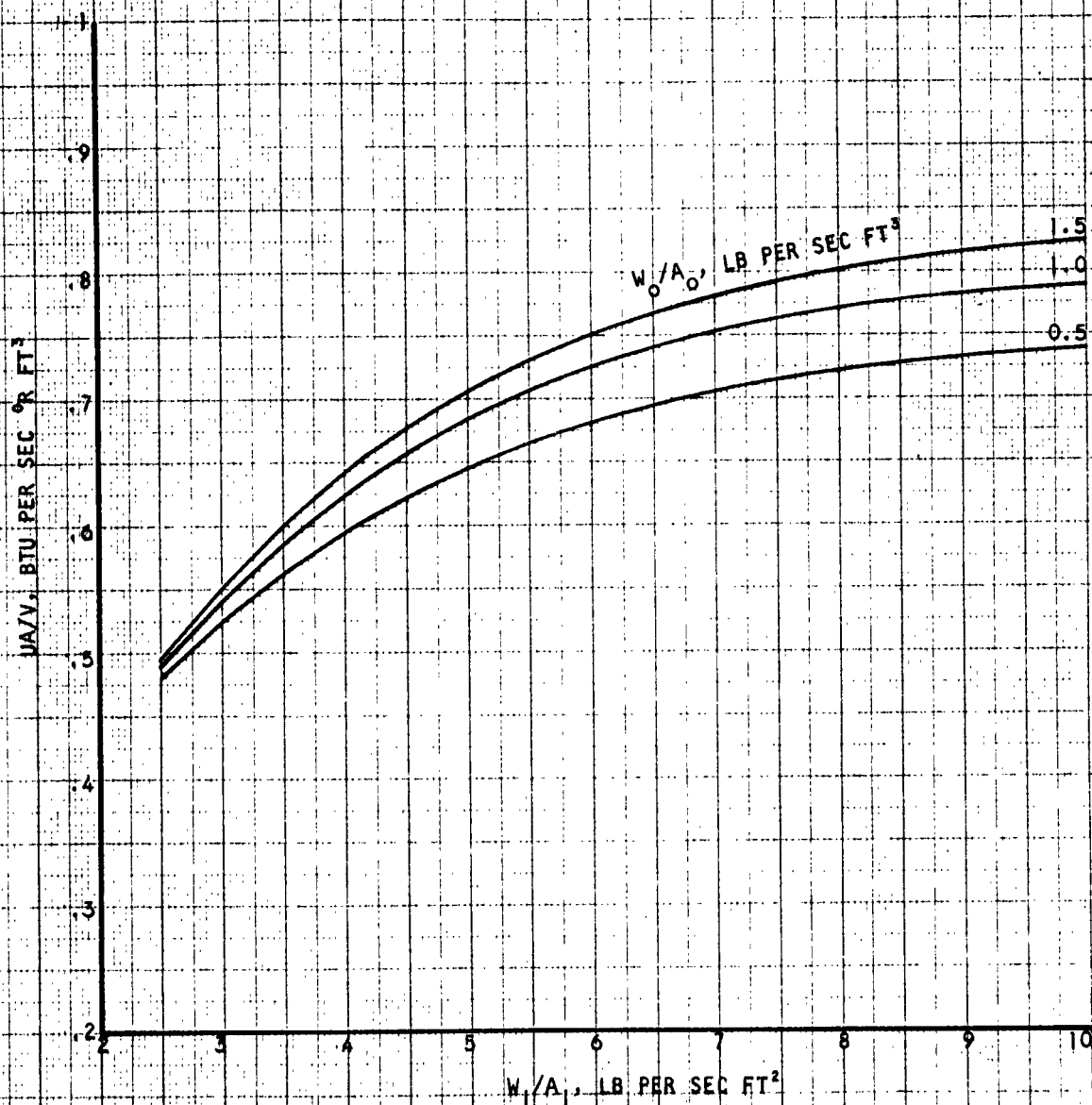




CALCULATED BY	FMW	8-62	RECUPERATOR DESIGN CURVES EXHAUST GAS INSIDE STRAIGHT TUBES  AIRESEARCH MANUFACTURING CO. LOS ANGELES CALIFORNIA	FIGURE 7-3
TRACED BY				
CHECKED BY				
APPROVED BY				
UNIT NO				



CALCULATED BY	FMW	8-62	RECUPERATOR DESIGN CURVES EXHAUST GAS INSIDE STRAIGHT TUBES	FIGURE 7-4
TRACED BY				
CHECKED BY			AIRESEARCH MANUFACTURING CO. LOS ANGELES - CALIFORNIA	
APPROVED BY				
UNIT NO				



CALCULATED BY	FMW	8-62
TRACED BY	FMW	8-62
CHECKED BY		
APPROVED BY		
UNIT NO.		

RECUPERATOR DESIGN CURVES  
EXHAUST GAS OUTSIDE  
PLAIN U-TUBES  
A RESEARCH MANUFACTURING CO.  
LOS ANGELES CALIFORNIA

FIGURE  
7-5

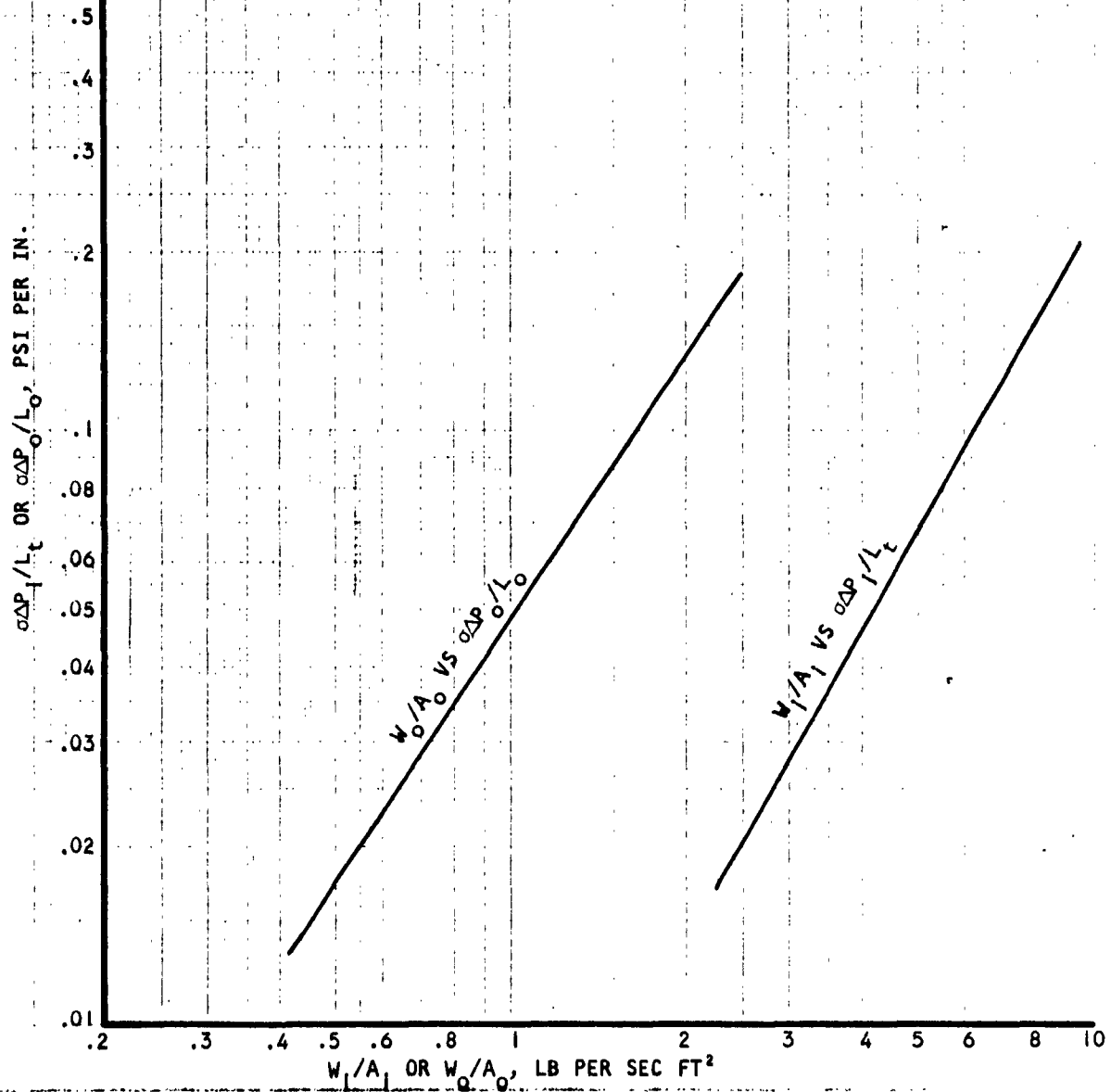


THE GARRETT CORPORATION  
A Research Manufacturing Division  
LOS ANGELES 48, CALIFORNIA

L-9149-R  
Page 68

**NOTE:**

$\alpha = \frac{\rho}{0.0765}$ , WHERE  $\rho$  = DENSITY IN LB PER CU FT AT AVERAGE PRESSURE AND TEMPERATURE



COORDINATED BY	FMW	8-62	RECUPERATOR DESIGN CURVES EXHAUST GAS OUTSIDE PLAIN U-TUBES	FIGURE 7-6
DESIGNED BY	FMW	8-62		
CHECKED BY			AIRESEARCH MANUFACTURING CO. LOS ANGELES, CALIFORNIA	
APPROVED BY				
DATE				

## SECTION 8

### SUMMARY

In summary, it is concluded that turboprop engine recuperators can be fabricated for aircraft where long endurance capability is required at part load engine operation. Compact lightweight tubular designs have been developed for this application. The most efficient tubular recuperator design is one in which the exhaust gas flows inside the tubes and the compressed air flows in two passes around the tubes (EIT), and this design has been selected for the Phase II recuperator endurance test. This choice resulted from evaluation of the two designs, treating the engine-recuperator combination as a complete system. The straight tube unit is lighter in core and wrap-up weight, shorter, and has a more desirable internal structure. Also, it is of less costly construction and easier to maintain. Development tests have demonstrated that this concept will be practical, reliable and economical to produce.

Comparing the (EIT) design with the U-tube design (EOT), it is noted that the gas side surfaces would be easier to clean and, since the gas side has relatively large open passages, there would be less of a tendency to build up deposits of combustion products. Actually, examination of both test units after all testing was completed showed that, other than heat discoloration, neither design had been fouled at all. This was in spite of the fact that, during the test program, fuel occasionally had leaked into the line and caused combustion to start briefly in the heat exchanger during shutdown.

The development of highly efficient tubular heat transfer surfaces during this program has made possible major reductions in the amount of heat transfer surface required, thus offering very attractive size and weight possibilities. It is possible that further investigation will also produce important savings in structural weight. It would appear that this, coupled with engine acceptance tests, would result in the production of a refined recuperator design within a reasonable period of time that would be a worthwhile, reliable addition to the present and future family of turboprop or turboshaft engines.

## SECTION 9

### PHASE II PROGRAM

By evaluation of the test data collected during Phase I, it is concluded that exhaust gas inside straight tubes in a recuperator of annular configuration will provide:

1. Lightest weight
2. Smallest volume
3. Suitable proportions
4. High reliability
5. Moderate cost
6. Adequate life
7. Ease of manufacture.

In Phase II, this type of recuperator design will be fabricated in a complete annulus and tested to determine life and structural integrity under flow, thermal, and pressure cyclic conditions.

Mounting interface problems will be considered and solutions will be offered.

## SECTION 10

### NOMENCLATURE

A	= core face area, ft <sup>2</sup>
a	= compressed air
C	= specific heat, Btu per lb °R
E	= effectiveness, $\frac{\Delta T_{\text{hot}} \text{ or } \Delta T_{\text{cold}}}{T_{\text{hot in}} - T_{\text{cold in}}}$ , dimensionless
(EIT)	= exhaust gas inside tubes
(EOT)	= exhaust gas outside tubes
f	= $\frac{\text{wt fuel}}{\text{wt air}}$ in exhaust gas, dimensionless
g	= exhaust gas
i	= inside tubes
ID	= core inside diameter, inches
Lo = $\frac{OD-ID}{2}$	= outside tubes flow length, inches
Ln = $(\frac{OD+ID}{2})\pi$	= no flow length, inches
Lt	= tube length between tube sheets, inches
o	= outside tubes
OD	= core outside diameter, inches
P	= pressure, psia
$\Delta P$	= pressure drop, psia
Total $\frac{\Delta P}{P_{\text{in}}}$	= $\frac{\Delta P_a}{P_{a \text{ in}}} + \frac{\Delta P_g}{P_{g \text{ in}}}$ , per cent
Q	= heat transfer rate, Btu per sec
T	= temperature, °R or °F
$\frac{UA}{V}$	= overall thermal conductance per unit volume of tube bundle, Btu per sec °R ft <sup>3</sup>
W	= flow rate, lb per sec

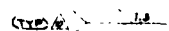


# NOMENCLATURE (CONTD)

X	= specific heat correction factor for combustion products, dimensionless
$\rho$	= density at average pressure and temperature, lb per ft <sup>3</sup>
$\sigma$	= $\frac{\rho}{0.0765}$ , dimensionless



NOTAL FOR 2020 &  
C/SINK FAR SIDE  
2019



**178123**

3/4" DIA 18 HOLES  
SEE ITEM 1

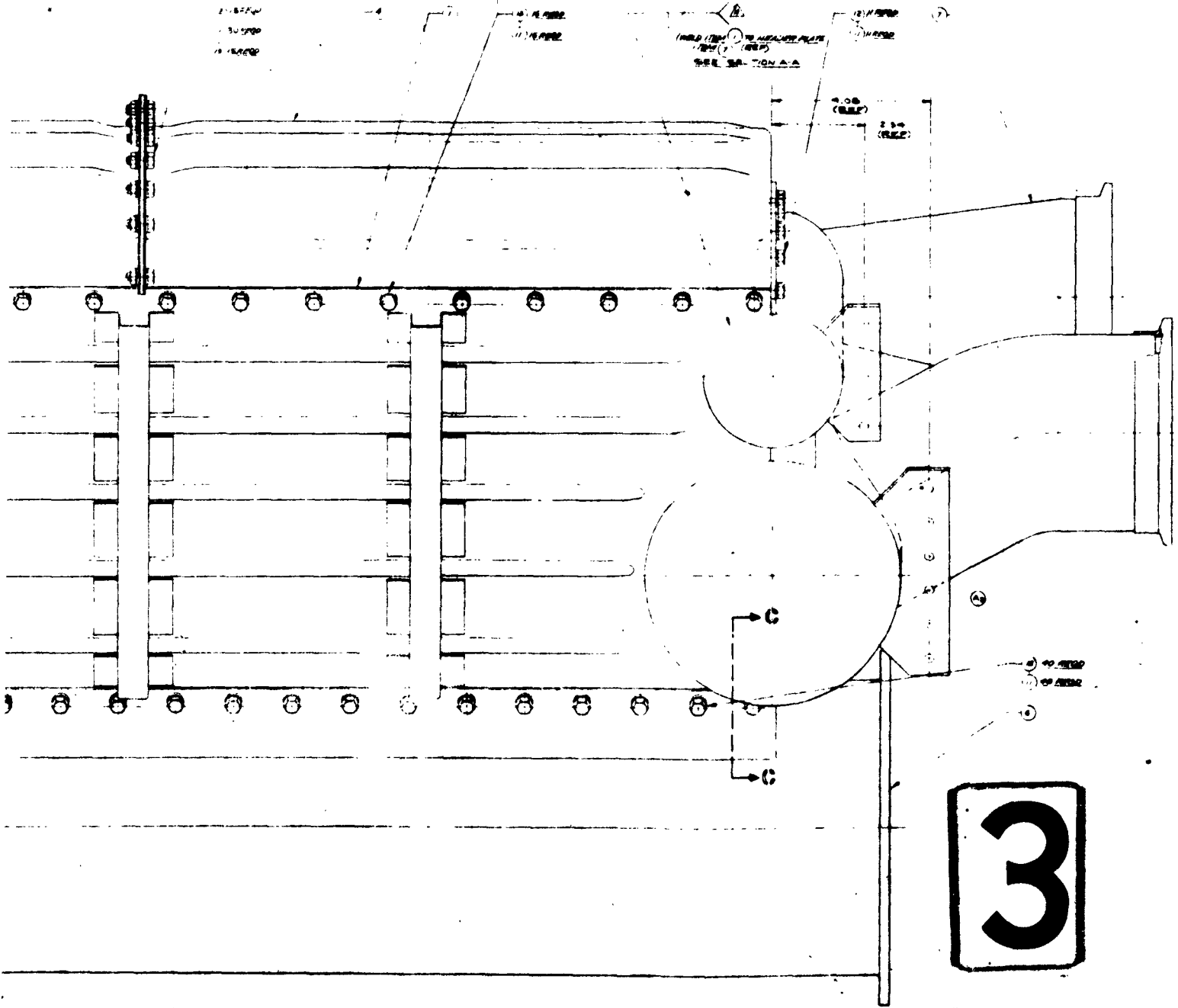
- TRANSFORMER ROOM (SEE SECTION 11-10000)  
IN ITEM 11-10000 COVER
- ① 1/2" DIA. INSTALL IN ITEM 11-10000
  - ② 1/4" DIA. INSTALL PER SECTION 11-10000

- DRILL 1/2" DIA. 18 HOLES  
IN TRANSFORMER ROOM COVER
- ③ 1/2" DIA. INSTALL IN TRANSFORMER ROOM COVER
  - ④ 1/4" DIA. INSTALL IN TRANSFORMER ROOM COVER
  - ⑤ 1/2" DIA. INSTALL PER SECTION 11-10000

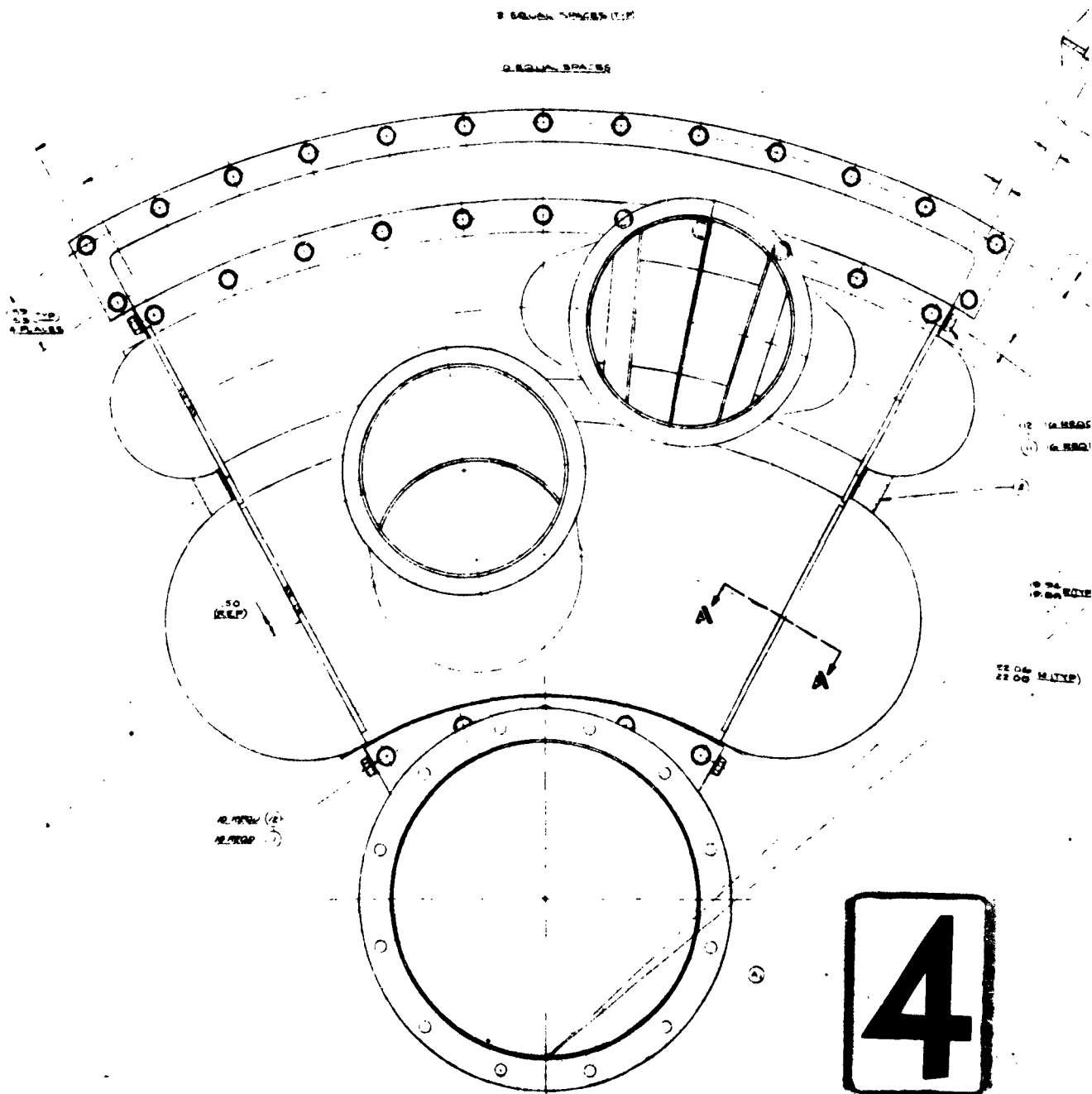
1/2" DIA  
1/4" DIA  
1/2" DIA

WELD TO HEAVY PLATE  
(SEE SECTION 11-10000)

2" DIA  
(SEE SECTION 11-10000)

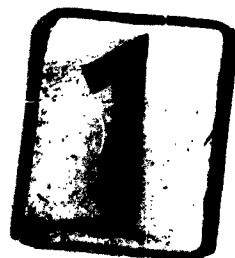
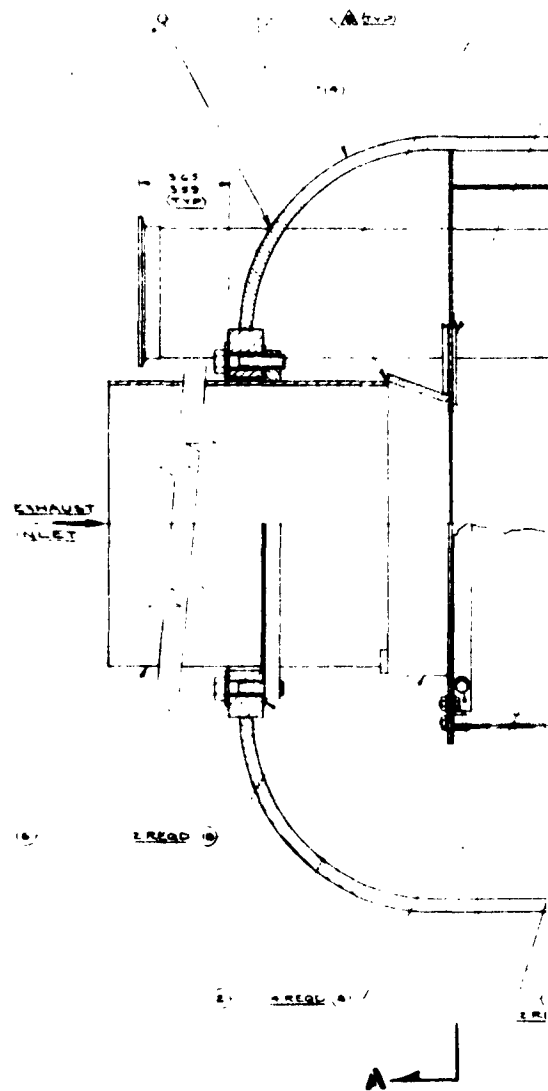
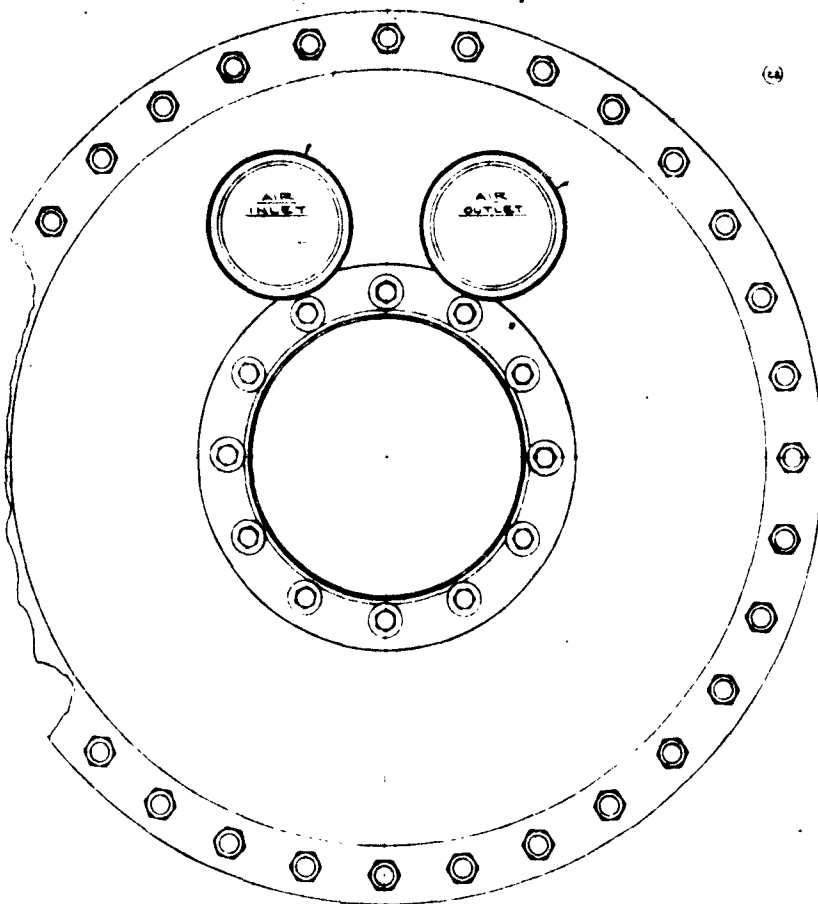


3



1997, 1998, 1999, 2000, 2001, 2002, 2003, 2004, 2005, 2006, 2007, 2008, 2009, 2010, 2011, 2012, 2013, 2014, 2015, 2016, 2017, 2018, 2019, 2020, 2021, 2022, 2023, 2024, 2025, 2026, 2027, 2028, 2029, 2030, 2031, 2032, 2033, 2034, 2035, 2036, 2037, 2038, 2039, 2040, 2041, 2042, 2043, 2044, 2045, 2046, 2047, 2048, 2049, 2050, 2051, 2052, 2053, 2054, 2055, 2056, 2057, 2058, 2059, 2060, 2061, 2062, 2063, 2064, 2065, 2066, 2067, 2068, 2069, 2070, 2071, 2072, 2073, 2074, 2075, 2076, 2077, 2078, 2079, 2080, 2081, 2082, 2083, 2084, 2085, 2086, 2087, 2088, 2089, 2090, 2091, 2092, 2093, 2094, 2095, 2096, 2097, 2098, 2099, 2100, 2101, 2102, 2103, 2104, 2105, 2106, 2107, 2108, 2109, 2110, 2111, 2112, 2113, 2114, 2115, 2116, 2117, 2118, 2119, 2120, 2121, 2122, 2123, 2124, 2125, 2126, 2127, 2128, 2129, 2130, 2131, 2132, 2133, 2134, 2135, 2136, 2137, 2138, 2139, 2140, 2141, 2142, 2143, 2144, 2145, 2146, 2147, 2148, 2149, 2150, 2151, 2152, 2153, 2154, 2155, 2156, 2157, 2158, 2159, 2160, 2161, 2162, 2163, 2164, 2165, 2166, 2167, 2168, 2169, 2170, 2171, 2172, 2173, 2174, 2175, 2176, 2177, 2178, 2179, 2180, 2181, 2182, 2183, 2184, 2185, 2186, 2187, 2188, 2189, 2190, 2191, 2192, 2193, 2194, 2195, 2196, 2197, 2198, 2199, 2200, 2201, 2202, 2203, 2204, 2205, 2206, 2207, 2208, 2209, 2210, 2211, 2212, 2213, 2214, 2215, 2216, 2217, 2218, 2219, 2220, 2221, 2222, 2223, 2224, 2225, 2226, 2227, 2228, 2229, 2230, 2231, 2232, 2233, 2234, 2235, 2236, 2237, 2238, 2239, 2240, 2241, 2242, 2243, 2244, 2245, 2246, 2247, 2248, 2249, 2250, 2251, 2252, 2253, 2254, 2255, 2256, 2257, 2258, 2259, 2260, 2261, 2262, 2263, 2264, 2265, 2266, 2267, 2268, 2269, 2270, 2271, 2272, 2273, 2274, 2275, 2276, 2277, 2278, 2279, 2280, 2281, 2282, 2283, 2284, 2285, 2286, 2287, 2288, 2289, 2290, 2291, 2292, 2293, 2294, 2295, 2296, 2297, 2298, 2299, 2300, 2301, 2302, 2303, 2304, 2305, 2306, 2307, 2308, 2309, 2310, 2311, 2312, 2313, 2314, 2315, 2316, 2317, 2318, 2319, 2320, 2321, 2322, 2323, 2324, 2325, 2326, 2327, 2328, 2329, 2330, 2331, 2332, 2333, 2334, 2335, 2336, 2337, 2338, 2339, 2340, 2341, 2342, 2343, 2344, 2345, 2346, 2347, 2348, 2349, 2350, 2351, 2352, 2353, 2354, 2355, 2356, 2357, 2358, 2359, 2360, 2361, 2362, 2363, 2364, 2365, 2366, 2367, 2368, 2369, 2370, 2371, 2372, 2373, 2374, 2375, 2376, 2377, 2378, 2379, 2380, 2381, 2382, 2383, 2384, 2385, 2386, 2387, 2388, 2389, 2390, 2391, 2392, 2393, 2394, 2395, 2396, 2397, 2398, 2399, 2400, 2401, 2402, 2403, 2404, 2405, 2406, 2407, 2408, 2409, 2410, 2411, 2412, 2413, 2414, 2415, 2416, 2417, 2418, 2419, 2420, 2421, 2422, 2423, 2424, 2425, 2426, 2427, 2428, 2429, 2430, 2431, 2432, 2433, 2434, 2435, 2436, 2437, 2438, 2439, 2440, 2441, 2442, 2443, 2444, 2445, 2446, 2447, 2448, 2449, 2450, 2451, 2452, 2453, 2454, 2455, 2456, 2457, 2458, 2459, 2460, 2461, 2462, 2463, 2464, 2465, 2466, 2467, 2468, 2469, 2470, 2471, 2472, 2473, 2474, 2475, 2476, 2477, 2478, 2479, 2480, 2481, 2482, 2483, 2484, 2485, 2486, 2487, 2488, 2489, 2490, 2491, 2492, 2493, 2494, 2495, 2496, 2497, 2498, 2499, 2500, 2501, 2502, 2503, 2504, 2505, 2506, 2507, 2508, 2509, 2510, 2511, 2512, 2513, 2514, 2515, 2516, 2517, 2518, 2519, 2520, 2521, 2522, 2523, 2524, 2525, 2526, 2527, 2528, 2529, 2530, 2531, 2532, 2533, 2534, 2535, 2536, 2537, 2538, 2539, 2540, 2541, 2542, 2543, 2544, 2545, 2546, 2547, 2548, 2549, 2550, 2551, 2552, 2553, 2554, 2555, 2556, 2557, 2558, 2559, 2560, 2561, 2562, 2563, 2564, 2565, 2566, 2567, 2568, 2569, 2570, 2571, 2572, 2573, 2574, 2575, 2576, 2577, 2578, 2579, 2580, 2581, 2582, 2583, 2584, 2585, 2586, 2587, 2588, 2589, 2590, 2591, 2592, 2593, 2594, 2595, 2596, 2597, 2598, 2599, 2600, 2601, 2602, 2603, 2604, 2605, 2606, 2607, 2608, 2609, 2610, 2611, 2612, 2613, 2614, 2615, 2616, 2617, 2618, 2619, 2620, 2621, 2622, 2623, 2624, 2625, 2626, 2627, 2628, 2629, 2630, 2631, 2632, 2633, 2634, 2635, 2636, 2637, 2638, 2639, 2640, 2641, 2642, 2643, 2644, 2645, 2646, 2647, 2648, 2649, 2650, 2651, 2652, 2653, 2654, 2655, 2656, 2657, 2658, 2659, 2660, 2661, 2662, 2663, 2664, 2665, 2666, 2667, 2668, 2669, 2670, 2671, 2672, 2673, 2674, 2675, 2676, 2677, 2678, 26





14 REQD (27) 12  
14 REQD (28) 12

ITEM 6 WELD AT ASSY TO PROVIDE FOR APPROX. 1/2 DEPLETION OF ITEM 10.

WELD 4 (222-242) DIA. 1/2 IN. TO FLANGE & ITEM 10.

1 REQD



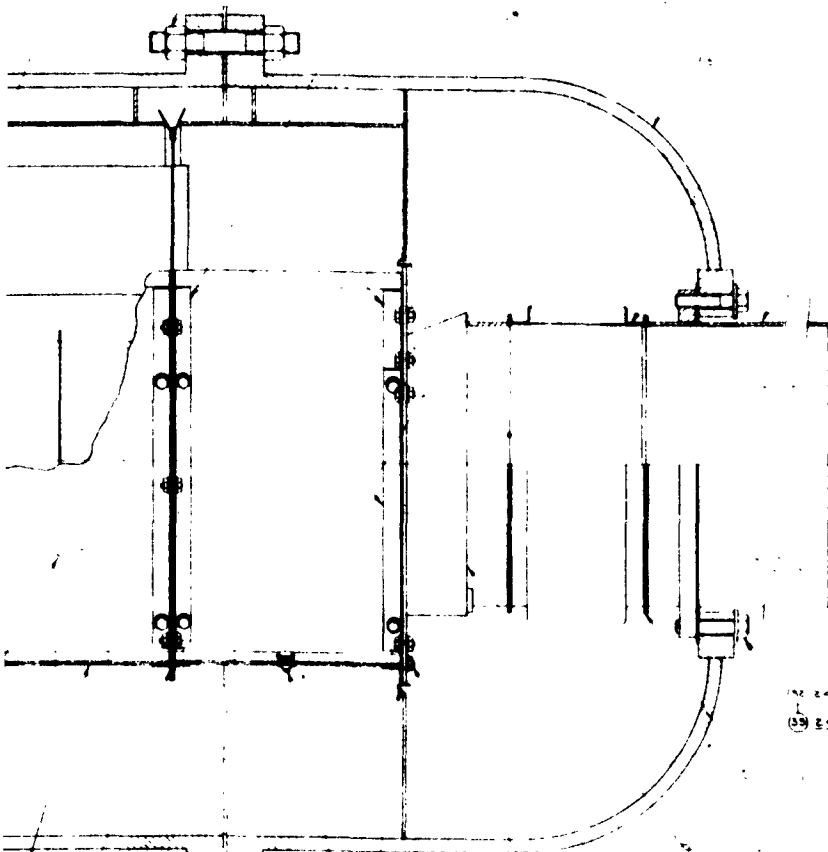
1 REQD  
1 REQD

1 REQD  
1 REQD

1 REQD

1 REQD  
1 REQD  
1 REQD

1 REQD



EXHAUST  
OUTLET

1 REQD  
1 REQD

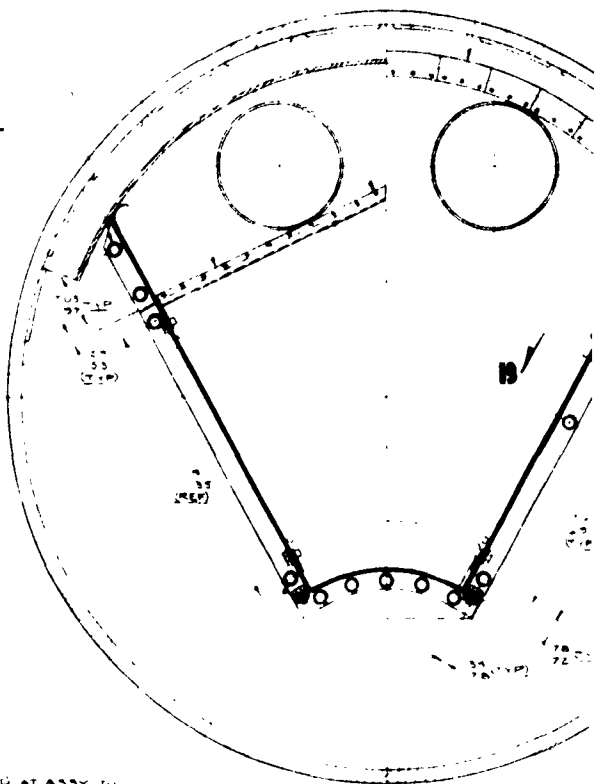
ITEM 6 WELD AT ASSY TO PROVIDE FOR APPROX. 1/2 DEPLETION OF ITEM 10.

WELD 4 (222-242) DIA. 1/2 IN. TO FLANGE & ITEM 10.

1 REQD  
1 REQD  
1 REQD

TRANSFER DRILL 4 (222-242) DIA. 1/2 IN. HOLES IN FLANGE & ITEM 10.

1 REQD  
1 REQD  
1 REQD



SECTION A-A

1 REQD  
1 REQD  
1 REQD

TRANSFER DRILL 4 (222-242) DIA. 1/2 IN. HOLES IN FLANGE & ITEM 10.

2

WELD PER AIRSEA WELDING PROC. 10.1  
WELD PER AIRSEA WELDING PROC. 10.1  
WELD PER AIRSEA WELDING PROC. 10.1

X178175



DRILL 2.55-2.58 DIA. 6 HOLES  
IN PLATE 1 ITEM 30121

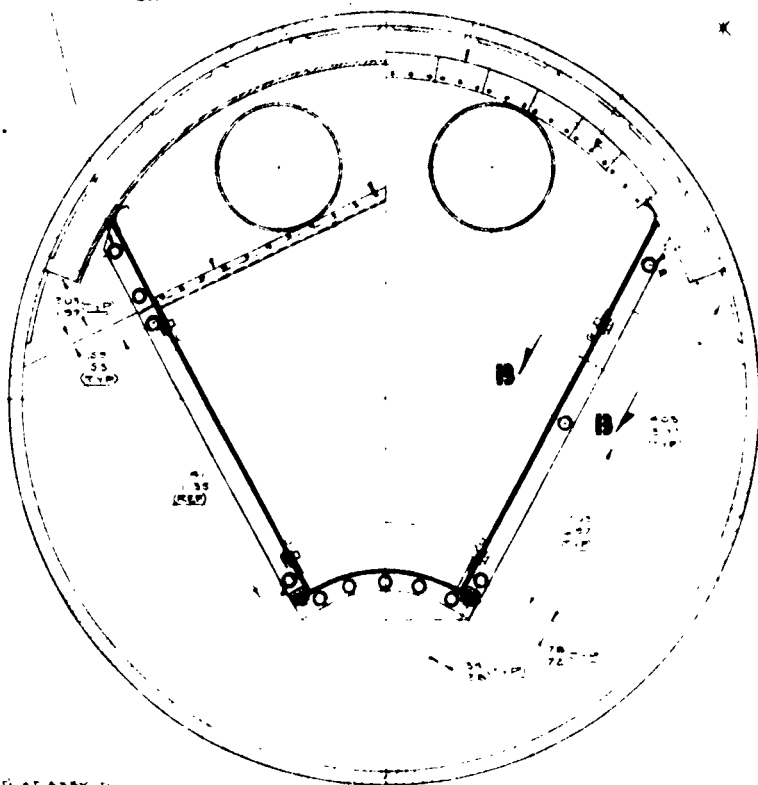
- (2) 1/2" HEAD
- (3) 1/2" HEAD
- (5) 1/2" HEAD

(7) 1/2" HEAD



SECTION B-B

(1) 1/2" HEAD



DRILL 2.55-2.58 DIA. 6 HOLES  
IN PLATE 1 ITEM 30121

- (2) 1/2" HEAD
- (3) 1/2" HEAD
- (5) 1/2" HEAD

3

WELD AT ASSY TO  
BE PLW APPROX  
APPROX 1/2" OF FORM  
APX

- (6) 1/2" HEAD
- (8) 1/2" HEAD
- (1) 1/2" HEAD

2.57 DIA. 6 HOLES  
ITEM 3

SECTION A-A

- ▲ NUT, STUD & WASHER DETAIL  
BY THE VENDOR
- ▲ PIT (TRIM) 1/2" MIN GAP  
BETWEEN ADJACENT ITEMS OF THE ASSY
- ▲ WELD PER AIRSEARCH SPEC VED 1
- ▲ WELD PER AIRSEARCH SPEC VED 1
- ▲ WELD PER AIRSEARCH SPEC VED 1
- ▲ WELD PER AIRSEARCH SPEC VED 1

ITEM 30121	WASHER	1
ITEM 30122	BOLT	1
ITEM 30123	NUT	1
ITEM 30124	WASHER	1
ITEM 30125	BOLT	1
ITEM 30126	NUT	1
ITEM 30127	DUCT ASSY	1
ITEM 30128	GUSSET	1
ITEM 30129	GUSSET	1
ITEM 30130	GUSSET	1
ITEM 30131	GUSSET	1
ITEM 30132	GUSSET	1
ITEM 30133	GUSSET	1
ITEM 30134	GUSSET	1
ITEM 30135	GUSSET	1
ITEM 30136	GUSSET	1
ITEM 30137	GUSSET	1
ITEM 30138	GUSSET	1
ITEM 30139	GUSSET	1
ITEM 30140	GUSSET	1
ITEM 30141	GUSSET	1
ITEM 30142	GUSSET	1
ITEM 30143	GUSSET	1
ITEM 30144	GUSSET	1
ITEM 30145	GUSSET	1
ITEM 30146	GUSSET	1
ITEM 30147	GUSSET	1
ITEM 30148	GUSSET	1
ITEM 30149	GUSSET	1
ITEM 30150	GUSSET	1
ITEM 30151	GUSSET	1
ITEM 30152	GUSSET	1
ITEM 30153	GUSSET	1
ITEM 30154	GUSSET	1
ITEM 30155	GUSSET	1
ITEM 30156	GUSSET	1
ITEM 30157	GUSSET	1
ITEM 30158	GUSSET	1
ITEM 30159	GUSSET	1
ITEM 30160	GUSSET	1
ITEM 30161	GUSSET	1
ITEM 30162	GUSSET	1
ITEM 30163	GUSSET	1
ITEM 30164	GUSSET	1
ITEM 30165	GUSSET	1
ITEM 30166	GUSSET	1
ITEM 30167	GUSSET	1
ITEM 30168	GUSSET	1
ITEM 30169	GUSSET	1
ITEM 30170	GUSSET	1
ITEM 30171	GUSSET	1
ITEM 30172	GUSSET	1
ITEM 30173	GUSSET	1
ITEM 30174	GUSSET	1
ITEM 30175	GUSSET	1
ITEM 30176	GUSSET	1
ITEM 30177	GUSSET	1
ITEM 30178	GUSSET	1
ITEM 30179	GUSSET	1
ITEM 30180	GUSSET	1
ITEM 30181	GUSSET	1
ITEM 30182	GUSSET	1
ITEM 30183	GUSSET	1
ITEM 30184	GUSSET	1
ITEM 30185	GUSSET	1
ITEM 30186	GUSSET	1
ITEM 30187	GUSSET	1
ITEM 30188	GUSSET	1
ITEM 30189	GUSSET	1
ITEM 30190	GUSSET	1
ITEM 30191	GUSSET	1
ITEM 30192	GUSSET	1
ITEM 30193	GUSSET	1
ITEM 30194	GUSSET	1
ITEM 30195	GUSSET	1
ITEM 30196	GUSSET	1
ITEM 30197	GUSSET	1
ITEM 30198	GUSSET	1
ITEM 30199	GUSSET	1
ITEM 30200	GUSSET	1

RECUPERATOR  
ASSY. TEST

70810 J170175